European Journal of Medicinal Chemistry 187 (2020) 111963

Contents lists available at ScienceDirect

European Journal of Medicinal Chemistry

journal homepage: http://www.elsevier.com/locate/ejmech

Research paper

Design and synthesis of novel ferrocene-quinoline conjugates and evaluation of their electrochemical and antiplasmodium properties

Aleksandra Minić [a, b, **], Tim Van de Walle [b], Kristof Van Hecke [c], Jill Combrinck [d, f], Peter J. Smith [d], Kelly Chibale [e], Matthias D'hooghe [b, *]

[a] Faculty of Technical Sciences, University of Priština, Knjaza Miloša 7, 38220, Kosovska Mitrovica, Serbia
[b] SynBioC Research Group, Department of Green Chemistry and Technology, Faculty of Bioscience Engineering, Ghent University, Coupure Links 653, B-9000, Ghent, Belgium
[c] XStruct, Department of Chemistry, Faculty of Sciences, Ghent University, Krijgslaan 281, S3, B-9000, Ghent, Belgium
[d] Medical School, University of Cape Town, K45, OMB, Groote Schuur Hopsital, Obervatory, 7925, South Africa
[e] South African Medical Research Council Drug Discovery and Development Research Unit, Department of Chemistry and Institute of Infectious Disease and Molecular Medicine, University of Cape Town, Rondebosch, 7701, South Africa
[f] Wellcome Centre for Infectious Diseases Research in Africa, Institute of Infectious Disease and Molecular Medicine, South Africa

ARTICLE INFO

Article history:
Received 16 September 2019
Received in revised form
26 November 2019
Accepted 10 December 2019
Available online 13 December 2019

Keywords:
Ferrocene
Quinolines
Cyclic voltammetry
Crystal structure
Antiplasmodium evaluation
Malaria

ABSTRACT

The tropical disease malaria is responsible for more than 400,000 deaths annually, especially in Southeast Asia and Africa. Although the number of malaria cases is declining, there still is an urgent need for novel antimalarial agents. The emergence of hybrid antimalarial agents and the precedence set by the antimalarial drug ferroquine (FQ) prompted us to design new ferrocene-containing quinoline structures. Herein, we report the efficient synthesis of three different series of ferrocene-quinoline conjugates and a class of ferrocene-containing heterotricycles in good to high yields. For all twenty novel ferrocenyl derivatives, electrochemical properties were investigated using cyclic voltammetry and antiplasmodium evaluation against a chloroquine-susceptible NF54 strain of the human malaria parasite *Plasmodium falciparum* was conducted, pointing to three compounds showing submicromolar potency. Subsequently, cytotoxicity assays against a Chinese Hamster Ovarian cell line and evaluation against a chloroquine-resistant strain of *Plasmodium falciparum* for these three compounds revealed selective and promising antiplasmodium activity.

1. Introduction

Malaria is a lethal parasitic infection caused by a protozoan parasitic disease, transmitted by *Anopheles* mosquitoes. In general, five species of the genus *Plasmodium* are known to provoke malarial infections in humans: *P. falciparum*, *P. vivax*, *P. malariae*, *P. ovale* and *P. knowlesi*, but the majority of cases is caused by *Plasmodium falciparum* (*P. falciparum*) and *Plasmodium vivax* (*P. vivax*) [1–5]. The life-threatening parasite *P. falciparum* is endemic in South and East Asia, South America, the Caribbean, the Middle East and Africa, whereas the non-lethal *P. vivax* prevails in Central America, India and parts of the Eastern Mediterranean. *P. ovale* and *P. malariae* are two rather rare, non-lethal parasites, most commonly found in Africa and Papua New Guinea [2]. Finally, in certain parts of Southeast Asia, *P. knowlesi* has been identified recently to induce a type of monkey malaria [6]. An estimated 219 million malaria cases were reported in 2017, resulting in 435,000 deaths. Especially Africa is affected by malaria, where mortality rates are highest (61%) in children under the age of five [7]. In addition, despite intensive investment in the development of a malaria vaccine, only limited success has been achieved in that respect [8]. Although several classes of antimalarial drugs are currently available, issues of toxicity, lower efficiency and resistance development by malaria parasites have reduced their overall therapeutic efficiency. Consequently, the search for new antimalarials remains an important challenge in drug discovery.

The use of metals to induce/enhance cytotoxicity of bioactive compounds has increased since the emergence of platinum-based

* Corresponding author.
** Corresponding author. Faculty of Technical Sciences, University of Priština, Knjaza Miloša 7, 38220, Kosovska Mitrovica, Serbia.
E-mail addresses: aleksandra.minic.989@gmail.com (A. Minić), Matthias.Dhooghe@UGent.be (M. D'hooghe).

https://doi.org/10.1016/j.ejmech.2019.111963
0223-5234/

chemotherapeutic agents for cancer treatment. In the context of antimalarial therapy, several metal-containing molecules have previously demonstrated to exert antiparasitic activity [8–12]. Ferroquine (FQ) (Fig. 1), a ferrocene-containing quinoline, has been developed as an important antimalarial agent and is currently in Phase II human clinical trials for uncomplicated *P. falciparum* malaria [3,13–15]. Designing new drugs based on FQ led to the preparation of numerous analogues, exemplified in Fig. 1 [13–16]. However, up to date, none of these analogues are able to compete with FQ in terms of antimalarial activity.

As a part of a project aimed at the preparation of new potentially bioactive ferrocene derivatives, we recently reported the synthesis of bioactive 2-ferrocenoyl ethyl aryl amines by aza-Michael additions of anilines across 1-ferrocenylpropenone [17,18]. 2-Ferrocenoyl ethyl aryl amines - Mannich bases - have proven to be excellent starting materials for further synthesis of ferrocene derivatives featuring a heterocyclic scaffold [19,20]. Bearing in mind all the above, we planned to synthesize a small library of ferrocenyl Mannich bases containing a quinoline core instead of a benzene ring in order to evaluate their antiplasmodium activity and use them for further synthetic transformations. Thus, herein we present the synthesis, structural and electrochemical characterization, as well as the pharmacological evaluation of three different sets of new ferrocene-quinoline conjugates: 1-ferrocenyl-3-(quinolinylamino)propan-1-ones, 1-ferrocenyl-3-(quinolinylamino) propan-1-ols, *N*-(3-ferrocenylprop-2-en-1-yl)-2,2,2-trifluoro-*N*-(quinolinyl)acetamides and a class of novel ferrocene-containing heterotricyclic products [21].

2. Results and discussion

2.1. Synthesis and structural characterization of novel ferrocene-containing compounds

The first step in our approach concerned the development of a suitable method for the synthesis of 1-ferrocenyl-3-(quinolinylamino)propan-1-ones. A few years ago, we designed and optimized reaction conditions for the synthesis of 3-arylamino-1-ferrocenylpropan-1-ones in high yields, which have been shown to be both biological active agents and excellent starting materials for further chemical modifications [17–20]. Thus, this protocol was adapted for the synthesis of our target compounds by using 4-aminoquinoline as the arylamino moiety (see Scheme 1). Unfortunately, after mixing 1 mmol of 1-ferrocenylpropenone **3** (synthesized *via* a previously described method [17–20]), 1.5 mmol of 4-aminoquinoline **4a** and 100 mg (0.42 mass equivalents) of montmorillonite K-10 clay in an ultrasound bath for 1 h, the desired compound could not be obtained (see Table 1, entry 1). Slight modifications of these conditions weren't satisfying either (see Table 1, entries 2–4), as the maximum yield that could be obtained *via* this method was 24% (see Table 1, entry 4), which was much lower compared with the previously synthesized 3-arylamino-1-ferrocenylpropan-1-ones *via* this protocol. These results prompted us to change our approach and to use aza-Michael additions of amines to enones, catalyzed by 0.1 M Na_2CO_3, as described by Xiao-Ji Tang et al. [22] Applying these conditions to the reaction (see Table 1, entry 5), we successfully synthesized 1-ferrocenyl-3-(quinolin-4-ylamino)propan-1-one **5a** in 19% yield. Again, we slightly varied and modified these reaction conditions (see Table 1, entries 6–7) and established the optimal parameters by augmenting the amount of Na_2CO_3 from 0.2 to 0.5 equivalents (see Table 1, entry 7). With the optimal conditions in hand, the scope of the reaction was investigated deploying four additional aminoquinolines **4b-e**, with a different substitution pattern. The products were obtained in good to excellent yields (up to 91%) after purification by means of column chromatography (SiO_2), as shown in Table 2. Structural characterization was made by spectroscopic methods (NMR, IR and MS) and revealed a purity of >95% for all derivatives.

The obtained amino ketones **5a-e** were then converted into the corresponding 1,3-amino alcohols. For the reduction of ketones **5**, $NaBH_4$ (five equivalents) in MeOH was employed, which lead to 1-ferrocenyl-3-(quinolinylamino)propan-1-ols **6a-e** in high yields (up to 98%), with short reaction times (see Schemes 2 and 3). Noteworthy, despite the efficient reduction process, all synthesized compounds had to be purified by column chromatography (SiO_2) to obtain products with a purity >95%, confirmed by NMR and LC-MS analysis. Because in general γ-amino alcohols represent versatile synthons in organic chemistry, the obtained ferrocene-containing

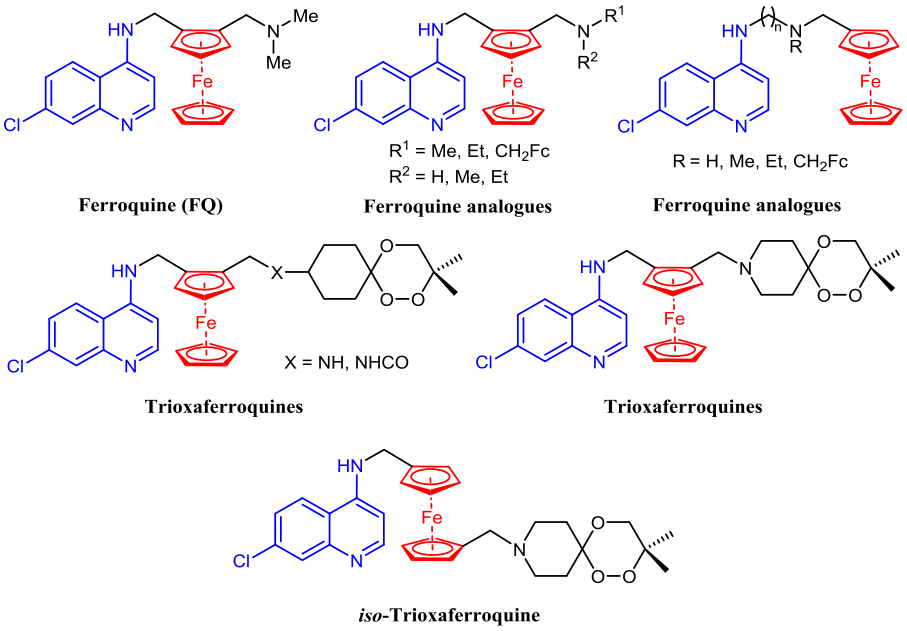

Fig. 1. Examples of some antimalarial quinolines bearing a ferrocene nucleus [13–16].

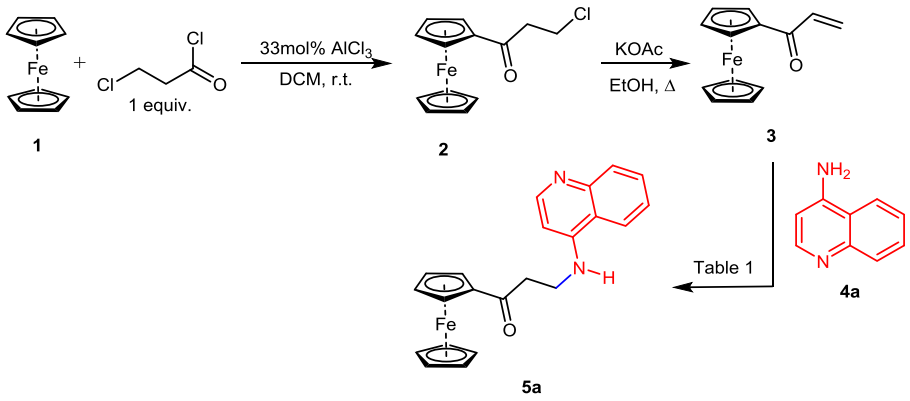

Scheme 1. Synthesis of 1-ferrocenyl-3-(quinolin-4-ylamino)propan-1-one **5a** starting from 1-ferrocenylpropenone **3** and 4-aminoquinoline **4a**.

Table 1
Attempts towards the synthesis of 1-ferrocenyl-3-(quinolin-4-ylamino)propan-1-one **5a**.

Entry	Catalyst	Eq. 4a	Time (h)	Yield (%)[a]
1	0.42 *m*-eq. montmorillonite K-10, ultrasound bath	1.5	1	/
2	0.42 *m*-eq. montmorillonite K-10, ultrasound bath	1.5	3	/
3	0.42 *m*-eq. montmorillonite K-10, ultrasound bath	1.5	5	Traces
4	0.42 *m*-eq. montmorillonite K-10, ultrasound bath	2	6	24
5	0.2 equiv. 0.1 M Na_2CO_3, Δ	2	14	19
6	0.2 equiv. 0.1 M Na_2CO_3, Δ	2	20	22
7	0.5 equiv. 0.1 M Na_2CO_3, Δ	2	16	57

[a] Isolated yields after purification.

Table 2
Substrate scope for the synthesis of 1-ferrocenyl-3-(quinolinylamino)propan-1-ones **5a-e**.

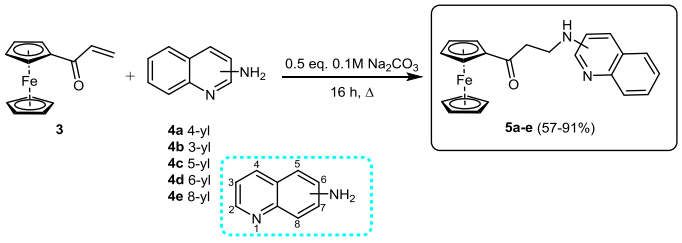

Entry	Substrate	Compound	Yield (%)[a]
1	**4a**	**5a**	57
2	**4b**	**5b**	71
3	**4c**	**5c**	90
4	**4d**	**5d**	87
5	**4e**	**5e**	91

[a] Isolated yields after purification.

1,3-amino alcohols, besides having promising biological activity themselves, represent excellent starting materials for further synthesis of ferrocene-containing compounds with interesting biological properties (antibacterial, antimalarial, anti-inflammatory, antitumor etc.) [23,24].

Therefore, the second part of our synthetic design comprised the evaluation of 1-ferrocenyl-3-(quinolinylamino)propan-1-ols **6** as substrates for the synthesis of functionalized ferrocene-containing quinoline conjugates, which represent new classes of compounds with great potential as biologically relevant structures (see Schemes 2 and 3). As mentioned in the introduction, ferrocene-quinoline conjugates are valuable new targets in medicinal chemistry, especially as antimalarial agents, because of the combined properties of the ferrocene moiety and the aminoquinoline core (as established antiplasmodium pharmacophores). Within that framework, we decided to transform 1-ferrocenyl-3-(quinolinylamino)propan-1-ols **6a-e** into unprecedented *N*-(3-ferrocenylprop-2-en-1-yl)-2,2,2-trifluoro-*N*-(quinolinyl)acetamides **7a-e** on the one hand and heterotricyclic products **8a-e** on the other hand, in order to evaluate the antiplasmodium activity of these two new compound classes as well.

A first route involved the transformation of 1-ferrocenyl-3-(quinolinylamino)propan-1-ols **6a-e** into *N*-(3-ferrocenylprop-2-en-1-yl)-2,2,2-trifluoro-*N*-(quinolinyl)acetamides **7a-e** upon treatment with triethylamine (1.5 equivalents) and trifluoroacetic anhydride (1.5 equivalents) in dry tetrahydrofuran at 0 °C (see Scheme 2, route b). Crude mixtures were purified by means of column chromatography (SiO_2) to afford amides **7a-e** in good yields (up to

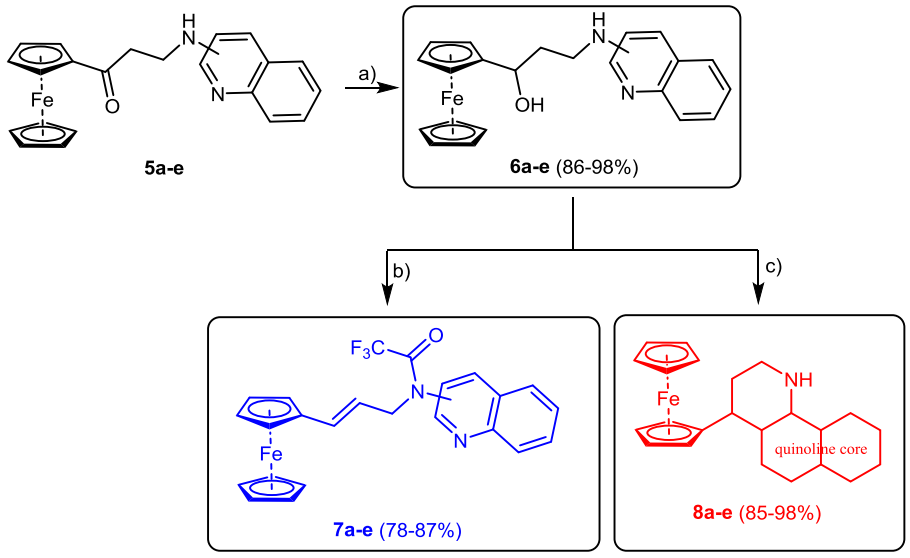

Scheme 2. Synthetic route to ferrocene-containing compounds **6**, **7** and **8**: (a) 5 equiv. $NaBH_4$, MeOH, 2 h, r.t., (b) 1.5 equiv. Et_3N, 1.5 equiv. $(CF_3CO)_2O$, dry THF, N_2 atmosphere, 16 h, 0 °C, (c) glacial acetic acid, ultrasound irradiation, 2 h, r.t.

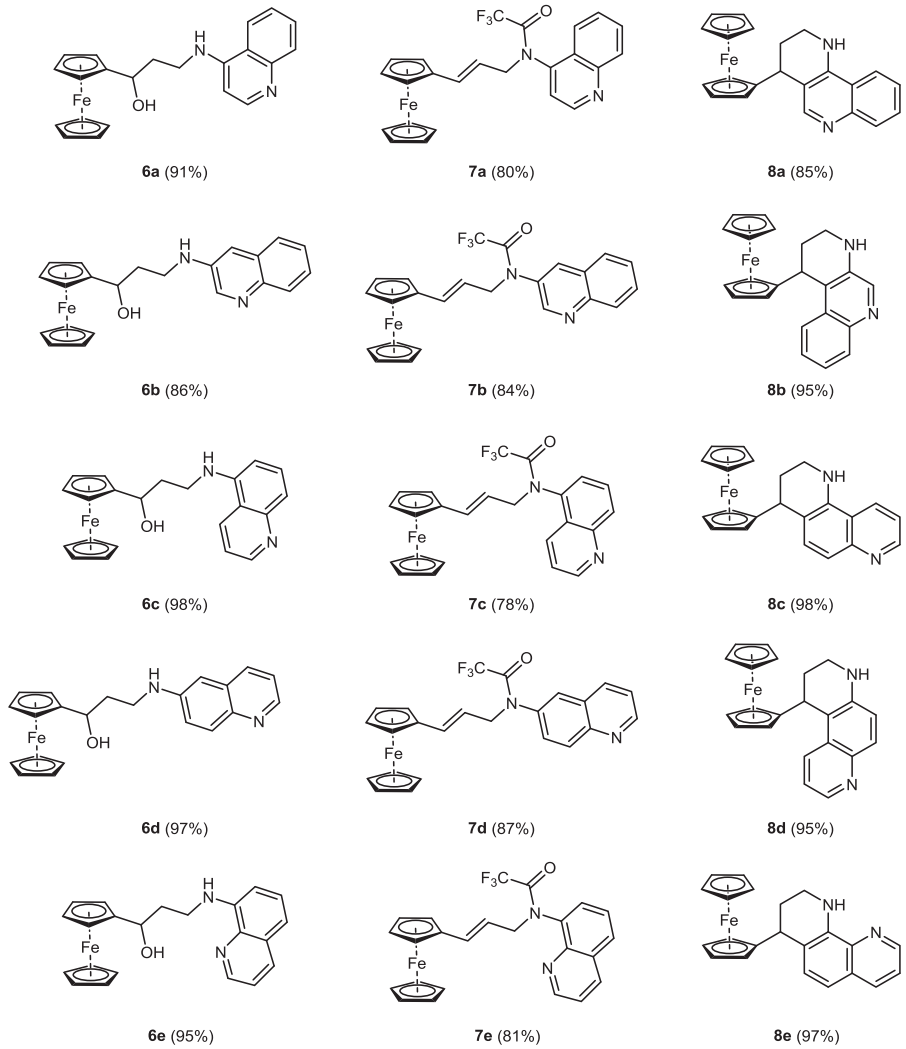

Scheme 3. Overview of synthesized new ferrocene-containing heterocycles **6**, **7** and **8**.

87%, see Scheme 3) and high purity (>95%, confirmed by NMR and LC-MS analysis). Based on ^{1}H NMR analysis, we concluded that all compounds **7a-e** possessed a double bond with *E*-configuration, since their olefinic protons showed a coupling constant of 15.5–15.6 Hz, which is a typical value for *E*-alkenes. Moreover, X-ray analysis was performed on a sample of compound **7d** (see Fig. 3), which revealed the presence of two invertomers with a different orientation of the three substituents around the aliphatic nitrogen atom due to hindered rotation.

In a second route, ferrocene-containing tricyclic compounds **8** were premised (see Scheme 2, route c). For this synthetic approach, a method previously reported by us was applied [20], which is efficient and requires mild reaction conditions. Results obtained by this transformation clearly show that 1-ferrocenyl-3-(quinolinylamino)propan-1-ols **6a-e** can smoothly undergo an intramolecular Friedel-Crafts-type reaction promoted by acetic acid, giving rise to the corresponding new heterotricycles **8a-e** in high to excellent yields (up to 98%, see Scheme 3).

For structures **6b** and **6d**, the formation of two cyclization products **8** is possible, because these compounds have two *ortho* positions relative to the amino functionality, which can give rise to two different positions for ring closure (see *ESI* Scheme S1 and Scheme S2). Interestingly, our study revealed that even though formation of two products was anticipated, in both cases only one product was obtained. The structures of **8b** and **8d** have been determined based on chemical shifts and coupling constants from the protons of the quinoline nucleus of the heterotricyclic part in ^{1}H NMR spectra, which in both cases could exclude the formation of the other predicted product (see Fig. 2 and experimental part). In addition, these results have been also confirmed using 2D NMR spectroscopy (HMBC, HSQC and NOESY, see *ESI*). Full confirmation of this set of heterotricyclic compounds **8** was obtained by means of NMR, IR and LC-MS analysis for all derivatives and X-ray analysis for compound **8e** (see Fig. 4).

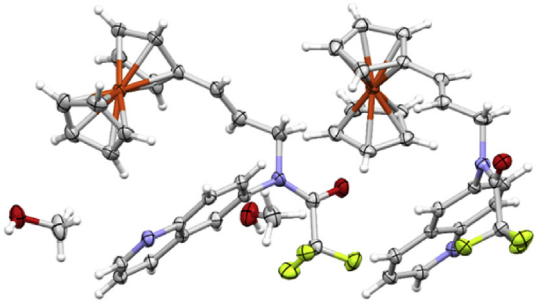

Fig. 3. Molecular structures of ferrocene-quinoline conjugate **7d**, showing thermal displacement ellipsoids at the 50% probability level.

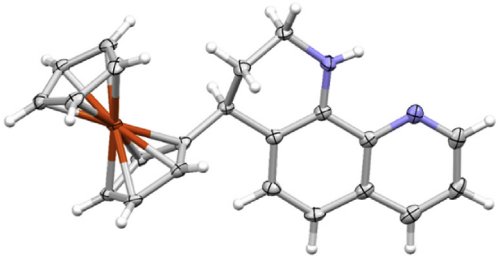

Fig. 4. Molecular structure of ferrocene-quinoline conjugate **8e**, showing thermal displacement ellipsoids at the 50% probability level.

2.2. Electrochemistry

It is well known that the Fe^{2+}/Fe^{3+} redox chemistry contributes to the bioactivity of ferrocene derivatives [17,19,26–29]. In view of that, we decided to evaluate the electrochemical properties of all newly synthesized compounds **5a-e**, **6a-e**, **7a-e** and **8a-e**. This was done by means of cyclic voltammetry (CV) in dichloromethane containing 0.1 mol/L tetrabutylammonium perchlorate as a supporting electrolyte. The working electrode was a polished (2mm diameter; Metrohm). The counter electrode was a platinum wire, whereas an Ag/AgCl electrode was used as the reference. The peak potentials (E_p) of the anodic and cathodic potentials (E_{pa} and E_{pc}, respectively, at 0.1 V s^{-1}), their half-wave potentials ($E_{1/2}$ =

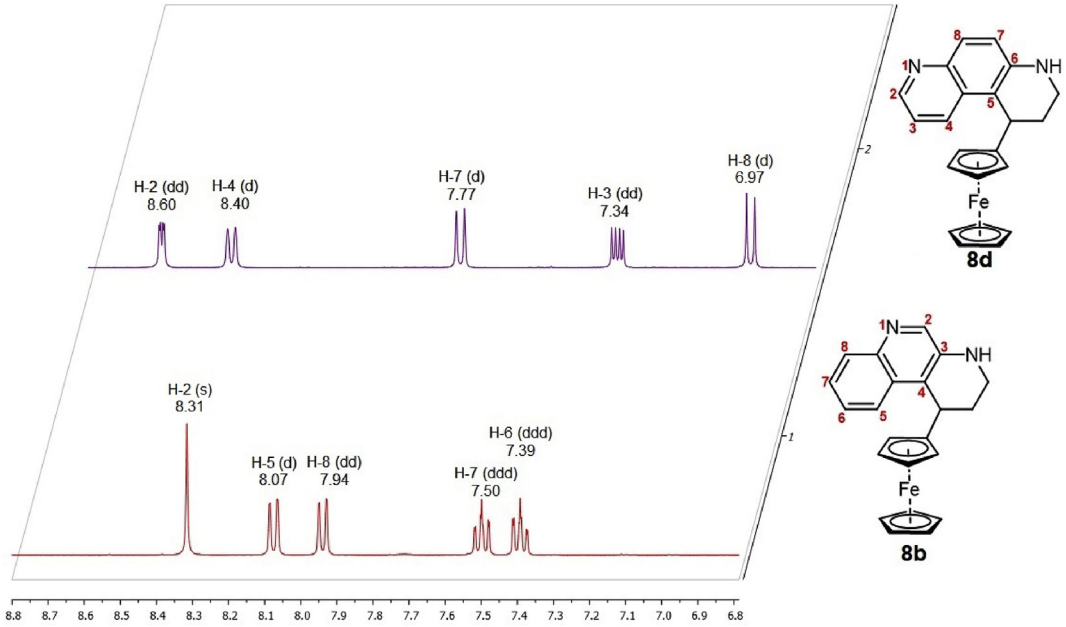

Fig. 2. Aromatic part of ^{1}H NMR spectra for compounds **8b** and **8d**.

(E_{pa} + E_{pc})/2), and the differences between anodic and cathodic peak potentials ($\Delta E = E_{pa} - E_{pc}$) of the ferrocenyl-derivatives 5a-e, **6a-e**, **7a-e** and **8a-e** are measured and evaluated as important electrochemical data [30]. All measurements were carried out using ferrocene as internal standard. In addition, CV measurements provide an additional proof of purity of our biologically investigated samples.

2.2.1. Electrochemical properties of 1-ferrocenyl-3-(quinolinylamino)propan-1-ones *5a-e*

The cyclic voltammogram of compound **5e** is shown (see Fig. 5 and *ESI* Fig. S10 and Fig. S11), as representative example, whereas the data for the other compounds are listed in Table 3. The 1-ferrocenyl-3-(quinolinylamino)propan-1-ones **5a-e** exhibit a reversible one-electron redox couple, as can be seen in Fig. 5. Oxidation wave (O1) appeared at 0.981 V, whereas the reduction wave (R1) showed up at 0.598 V, and we attributed them to the oxidation of the ferrocene unit during the forward-potential sweep, and the reduction of the obtained ferricenium ion at the back-potential sweep. It appears that the oxidation potentials of **5a-e** are considerably more positive than the ones of the unsubstituted ferrocenes ($Fc^+/Fc = 0.640$ V), which can be expected for ferrocene derivatives possessing an electron-withdrawing group conjugated to the cyclopentadienyl ring(s) [17,19,25]. This result shows significant electronic contact between the ferrocenyl units and the rest of the molecule. In addition, calculated ΔE (>0.250 V) for compounds **5a-e** are higher than the theoretical value (ΔE = 0.150 V) for reversible couples, which indicates the quasi-reversible nature of the system [30] also observed in similar monoferrocenyl derivatives [17,19,25].

2.2.2. Electrochemical properties of 1-ferrocenyl-3-(quinolinylamino)propan-1-ols *6a-e*

Data obtained from electrochemical evaluation of 1-ferrocenyl-3-(quinolinylamino)propan-1-ols **6a-e** are summarized in Table 4. All ferrocene-containing amino alcohols exhibit two well-defined oxidation waves on the forward-potential sweep (O2, at around 0.650 V and O3, at around 0.888 V, respectively) and one reduction wave during the back-potential sweep (R2, at around 0.345 V). The representative cyclic voltammograms recorded for compound 6e are illustrated in Fig. 6 (see also *ESI* Fig. S12). As it can be seen, the first oxidation peak (O2) occurred at 0.650 V while the corresponding anodic (R2) signal appeared at 0.345 V (see Fig. 6). We believe that these peaks correspond to the same redox couple, probably ferrocene/ferrocenium. It is noteworthy that if we compare forward-potential sweep oxidation waves of **6a-e** (O2 at around 0.650 V) with **5a-e** (O1 at around 0.981 V) and with the ones of the unsubstituted ferrocenes (Fc^+/Fc = 0.640 V), we can show the influence of the carbonyl group and hydroxyl group (bonded onto the α-ferrocenyl carbon atom) on the values of oxidation potentials [17,19,25]. On the other hand, the second oxidation wave (O3) is occurring due to an irreversible

Table 3
The electrochemical data for compounds **5a**-**e**.

Compound	E_{pa1} (V)[a]	E_{pc1} (V)[a]	$E_{1/2}$ (V)[b]	ΔE (V)[c]
5a	0.909	0.647	0.778	0.262
5b	0.919	0.653	0.786	0.266
5c	0.909	0.644	0.777	0.265
5d	0.928	0.656	0.792	0.272
5e	0.981	0.598	0.790	0.383

[a] E_{pa} and E_{pc} anodic and cathodic peak potentials, respectively, at 0.1 V s^{-1}
[b] $E_{1/2} = (E_{pa1} + E_{pc1})/2$.
[c] $\Delta E = E_{pa1} - E_{pc1}$.

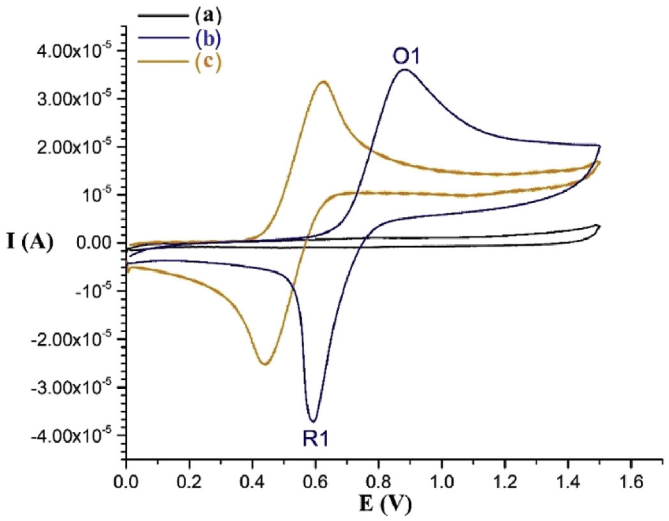

Fig. 5. Cyclic voltammograms at the platinum disk (d = 2 mm) by a 0.1 V s^{-1} scan rate in 0.1 M dichloromethane solution of Bu_4NClO_4: (a) electrolyte, (b) 1-ferrocenyl-3-(quinolin-8-ylamino)propan-1-one (**5e**), (c) ferrocene.

Table 4
The electrochemical data for compounds **6a**-**e**.

Compound	E_{pa2} (V)[a]	E_{pa3} (V)[a]	E_{pc2} (V)[a]	$E_{1/2}$ (V)[b]	ΔE (V)[c]
6a	0.571	1.105	0.427	0.499	0.144
6b	0.623	1.074	0.381	0.502	0.242
6c	0.613	0.943	0.385	0.499	0.228
6d	0.595	0.967	0.406	0.501	0.189
6e	0.650	0.888	0.345	0.498	0.305

[a] E_{pa} and E_{pc} anodic and cathodic peak potentials, respectively, at 0.1 V s^{-1}
[b] $E_{1/2} = (E_{pa2} + E_{pc2})/2$.
[c] $\Delta E = E_{pa2} - E_{pc2}$.

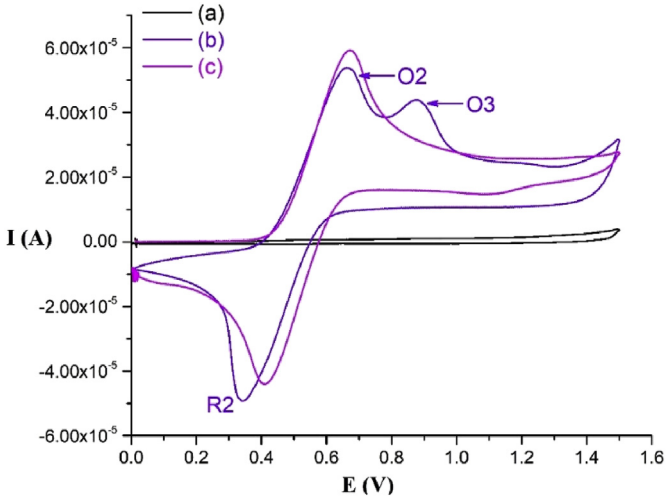

Fig. 6. Cyclic voltammograms at the platinum disk (d = 2 mm) by a 0.1 V s^{-1} scan rate in 0.1 M dichloromethane solution of Bu_4NClO_4: (a) electrolyte, (b) 1-ferrocenyl-3-(quinolin-8-ylamino)propan-1-ol (**6e**), (c) ferrocene.

electrochemical event. The origin of this second oxidation wave (O3) is established by linking structure and electrochemical properties of compounds **5a-e** with **6a-e**, and it can be assigned to the oxidation of the hydroxyl group. The voltammograms of **6e** at both higher and lower scan rates also contained peak O3 (see *ESI* Fig. S13), suggesting the stability of the oxidized species in solution

over a longer period.

2.2.3. Electrochemical properties of N-(3-ferrocenylprop-2-en-1-yl)-2,2,2-trifluoro-N-(quinolinyl)acetamides **7a-e**

The redox behavior of the products **7a-e** was determined using cyclic voltammetry (CV) under the same conditions mentioned above, and the results of this study are listed in Table 5. Based on these data, we can conclude that all novel ferrocene-containing derivatives **7a-e** exhibit one well-defined oxidation wave on the forward-potential sweep (O4 at 0.671–0.933 V) and one reduction wave during the back-potential sweep (R3 at 0.348–0.491 V), attributed to the ferrocene moiety. As a representative example, we present the cyclic voltammogram of compound **7b** (see Fig. 7 and *ESI* Fig. S14). Due to the reversibility of this electron transfer, even at low scan speed, the produced radical anion is stable within the time scale of cyclic voltammetry (see *ESI* Fig. S15) [30]. Moreover, the average of anodic and cathodic current was not unity and the difference between the oxidation and reduction maxima ($\Delta E = E_{pa4} - E_{pc3}$) was around 0.355. Compared with the theoretical value $\Delta E = 0.150$ V, we can confirm the quasi-reversible nature of the system [30].

2.2.4. Electrochemical properties of ferrocene-containing tricyclic products **8a-e** [21]

The voltammogram of compound **8b** is presented in Fig. 8, as representative example, whereas the data of the other compounds **8a-e** are listed in Table 6. As it can be seen from the summarized data, derivatives **8a-d** exhibit one well-defined oxidation wave on the forward potential sweep (O5, at 0.592–0.653 V) and one reduction wave on the back-potential sweep (R5, at 0.403–0.476 V). Since the difference between the values of these two potentials is close to the theoretical one, O5 and R5 apparently belong to a reversible redox couple, appearing due to the presence of the ferrocene nucleus [17,19,25,29]. Noteworthy, a considerable difference is observed for compound **8e** (see Table 6). Therefore, the cyclic voltammogram recorded for **8e** is shown in Fig. 9. Apparently, **8e** exhibit two well-defined oxidation waves on the forward potential sweep (O5, at 0.626 V and O6, at 0.940 V, respectively) and two reduction waves on the back-potential sweep (R4, at 0.659 V and R5, at 0.403 V, respectively). Considering the reversibility of ferrocene oxidation, the first redox couple (O5 and R5) certainly can be assigned to the metallocene moiety. On the other hand, the origin of the second redox wave is difficult to determine precisely, but it could potentially be correlated with the redox process of the tricyclic scaffold. The electrochemical properties of these series of ferrocenyl derivatives **8a-e** are highly interesting and warrant additional investigation [30], albeit both the extent and the type of further investigations are beyond the scope of this work.

2.3. Antiplasmodium activities

With this small library of ferrocene-quinolines and ferrocene-containing heterotricyclic derivatives in hand, pharmacological screening was performed. All 20 ferrocene derivatives were subjected to antiplasmodium testing. For the antiplasmodium assay, all samples were tested in triplicate against a chloroquine-sensitive (CQS) strain of *Plasmodium falciparum* (NF54). Subsequently,

Table 5
The electrochemical data for compounds **7a**-**e**.

Compound	E_{pa4} (V)[a]	E_{pc3} (V)[a]	$E_{1/2}$ (V)[b]	ΔE (V)[c]
7a	0.671	0.491	0.581	0.180
7b	0.781	0.430	0.606	0.351
7c	0.933	0.348	0.641	0.585
7d	0.732	0.449	0.591	0.283
7e	0.812	0.439	0.626	0.373

[a] E_{pa} and E_{pc} anodic and cathodic peak potentials, respectively, at 0.1 V s^{-1}
[b] $E_{1/2} = (E_{pa4} + E_{pc3})/2$.
[c] $\Delta E = E_{pa4} - E_{pc3}$.

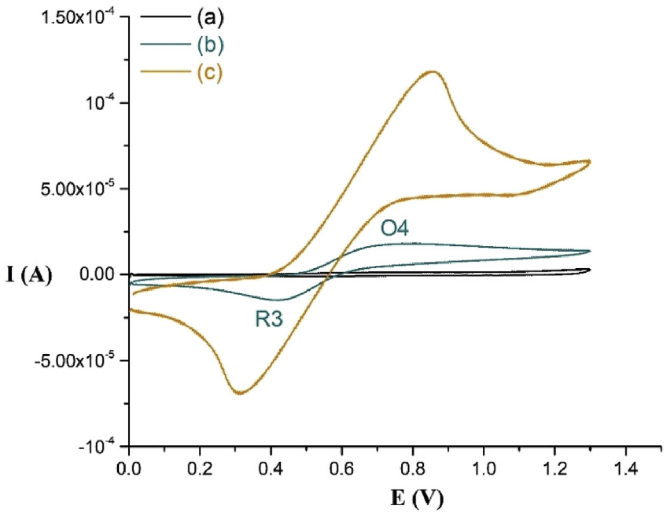

Fig. 7. Cyclic voltammograms at the platinum disk (d = 2 mm) by a 0.1 V s^{-1} scan rate in 0.1 M dichloromethane solution of Bu_4NClO_4: (a) electrolyte, (b) *N*-(3-ferrocenylprop-2-en-1-yl)-2,2,2-trifluoro-*N*-(quinoline-3-yl)acetamide (**7b**), (c) ferrocene.

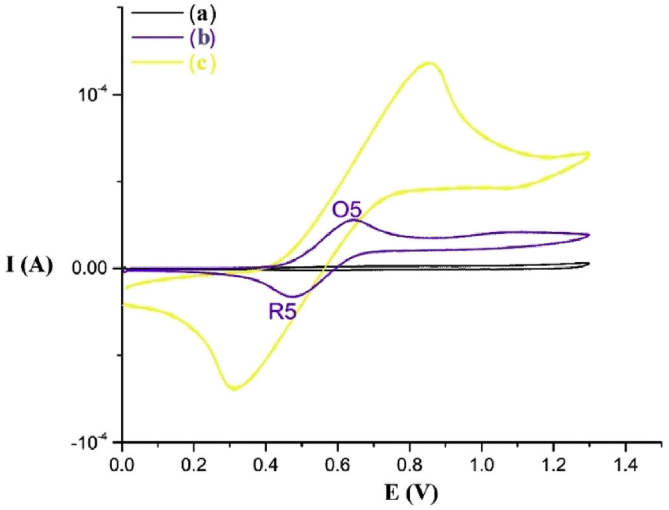

Fig. 8. Cyclic voltammograms at the platinum disk (d = 2 mm) by a 0.1 V s^{-1} scan rate in 0.1 M dichloromethane solution of Bu_4NClO_4: (a) electrolyte, (b) 1-Ferrocenyl-1,2,3,4-tetrahydrobenzo[f] [1,7]naphthyridine (**8b**), (c) ferrocene.

Table 6
The electrochemical data for compounds **8a**-**e**.

Compound	E_{pa5} (V)[a]	E_{pa6} (V)[a]	E_{pc4} (V)[a]	E_{pc5} (V)[a]	$E_{1/2}$ (V)[b]	ΔE (V)[c]
8a	0.641	–	–	0.476	0.559	0.174
8b	0.592	–	–	0.470	0.531	0.122
8c	0.641	–	–	0.458	0.550	0.183
8d	0.653	–	–	0.406	0.530	0.247.
8e	0.626	0.940	0.659	0.403	0.515	0.223

[a] E_{pa} and E_{pc} anodic and cathodic peak potentials, respectively, at 0.1 V s^{-1}
[b] $E_{1/2} = (E_{pa5} + E_{pc5})/2$.
[c] $\Delta E = E_{pa5} - E_{pc5}$.

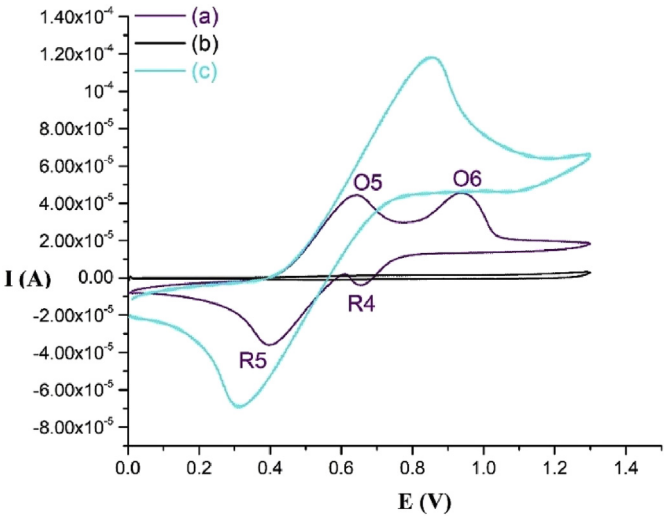

Fig. 9. Cyclic voltammograms at the platinum disk (d = 2 mm) by a 0.1 V s^{-1} scan rate in 0.1 M dichloromethane solution of Bu_4NClO_4: (a) electrolyte, (b) 4-Ferrocenyl-1,2,3,4-tetrahydro-1,10-phenanthroline (**8e**), (c) ferrocene.

samples that showed promising antiplasmodium activity (i.e. compounds **5a**, **6a** and **7a**) were tested in triplicate against a chloroquine-resistant (CQR) strain of *P. falciparum* (K1) and screened for *in vitro* cytotoxicity against a mammalian cell-line, Chinese Hamster Ovarian (CHO), using the 3-(4,5-dimethylthiazol-2-yl)-2,5-diphenyltetrazolium bromide (MTT)-assay, also in triplicate. Chloroquine was used as a reference compound in the antiplasmodium assays, whereas the antiprotozoal agent emetine was used in the cytotoxicity tests as positive control. Continuous *in vitro* cultures of asexual erythrocyte stages of *P. falciparum* were maintained using a modified method of Trager and Jensen [31]. Quantitative assessment of antiplasmodium activity *in vitro* was determined *via* the parasite lactate dehydrogenase assay using a modified method described by Makler [32]. The MTT-assay was used as colorimetric assay to measure cell growth and survival and compares well with other available assays [33,34]. The results of the biological evaluation are summarized in Tables 7 and 8.

It can be seen that various analogues show weak to good activities (IC_{50} < 10 μM), with three of the tested compounds showing submicromolar (IC_{50} < 1 μM) potencies against a chloroquine-sensitive NF54 strain of *P. falciparum* (with IC_{50} values between 390 and 930 nM). However, ferrocene-containing heterotricyclic derivatives gave no significant activity (except derivative **8a**, IC_{50} = 1.69 μM). Subsequently, the activity of the three most potent compounds (**5a**, **6a** and **7a**) was determined against a chloroquine-resistant strain of *P. falciparum* (K1), which resulted in promising activities with IC_{50} values of 3.91, 0.77 and 0.82 μM, respectively (see Table 8). Moreover, these three derivatives also displayed a good cytotoxicity profile (lower activities against CHO, resulting in high selectivity indices). Regarding the structure-activity relationships, this assay shows that the best activities are obtained when ferrocene is linked to the quinoline ring at position 4, since compounds **5a**, **6a**, **7a** and **8a** are the four most potent compounds. Next to that, compounds **6a** and **7a** possess a lower (so a better) Resistance Index than compound **5a**, bearing a keto functional group. On the other hand, derivative **5a** has the best Selectivity Index. Due to the diversity of this library (focusing on various substitution patterns across the quinoline core and also the linker between ferrocene and quinoline ring), these results cannot be generalized, but they can be seen as a valuable starting point for further research on 4-functionalized ferrocene-quinolines.

Table 7
IC_{50} values for ferrocene-quinolines (**5**, **6**, and **7**) and ferrocene-containing heterotricyclic derivatives (**8**) tested for *in vitro* antimalarial activity against a CQS *P. falciparum* strain. Data are expressed as mean ± SD values of three independent experiments.

Compound	NF54: IC_{50} (μM)	Compound	NF54: IC_{50} (μM)
5a	0.85 ± 0.25	**7a**	0.93 ± 0.15
5b	5.75 ± 0.21	**7b**	12.18 ± 0.50
5c	3.13 ± 0.33	**7c**	19.26 ± 1.59
5d	5.36 ± 1.16	**7d**	17.47 ± 4.58
5e	27.79 ± 0.91	**7e**	12.21 ± 0.42
6a	0.39 ± 0.01	**8a**	1.69 ± 0.35
6b	5.63 ± 0.68	**8b**	82.76 ± 17.53
6c	3.99 ± 1.26	**8c**	22.35 ± 2.02
6d	9.65 ± 0.75	**8d**	39.49 ± 2.26
6e	21.08 ± 3.29	**8e**	30.44 ± 4.78
		CQ	0.011 ± 0.001
		FQ	0.029 ± 0.001

CQ = chloroquine.
FQ = ferroquine.

Table 8
IC_{50} values of ferrocene-quinolines **5a**, **6a** and **7a** tested for *in vitro* antimalarial activity (against a CQR *P. falciparum* strain) and cytotoxicity. Data are expressed as mean ± SD values of three independent experiments.

Compound	NF54: IC_{50} (μM)	K1: IC_{50} (μM)	CHO: IC_{50} (μM)	SI[a]	RI[b]
5a	0.85 ± 0.25	3.91 ± 0.07	251.68 ± 12.10	296.2	4.6
6a	0.39 ± 0.01	0.77 ± 0.07	23.14 ± 1.71	59.3	2.0
7a	0.93 ± 0.15	0.82 ± 0.05	19.90 ± 1.99	21.5	0.9
CQ	0.011 ± 0.001	0.167 ± 0.028	–	–	14.7
FQ	0.029 ± 0.001	0.039 ± 0.003	–	–	1.3
Emetine (μM)	–	–	0.04 ± 0.01	–	–

CQ = chloroquine.
FQ = ferroquine.
[a] SI (Selectivity Index) = IC_{50} CHO/IC_{50} NF54.
[b] RI (Resistance Index) = IC_{50} K1/IC_{50} NF54.

3. Conclusion

Preparation of three series of novel ferrocene-quinoline hybrids and ferrocene-containing heterotricycles was achieved using a simple and efficient synthetic protocol. Structures of novel compounds were confirmed by standard spectral techniques (NMR, IR and MS), and the proposed structures of two representative products **7d** and **8e** were also secured by single-crystal X-ray diffraction analysis. The cyclic voltammetry studies confirmed the previously reported correlation between electrochemical behavior and the biological activity of ferrocenes and revealed that derivatives **5a-e** and **7a-e** showed a single-electron reversible oxidation behavior attributed to the ferrocene nucleus, whereas products **6a-e** exhibited two well-defined oxidation waves and one reduction wave (O2 and R2 assigned to the metallocene unit and O3 assigned to the hydroxy group). Electrochemical evaluation of compounds **8a-e** showed that products **8a-d** exhibited only one well-defined redox couple (attributed to the ferrocene nucleus), whereas product **8e** exhibited two well-defined redox couples.

Furthermore, the *in vitro* antiplasmodium activity and cytotoxicity of the novel ferrocene-containing compounds was evaluated. Compounds **5a**, **6a** and **7a** displayed low micromolar activity against a chloroquine-sensitive strain of *P. falciparum*, and compounds **6a** and **7a** also exhibited a submicromolar activity against a chloroquine-resistant strain of *P. falciparum* with IC_{50}-values of 0.77 and 0.82 μM, respectively, accompanied by low cytotoxicity. In view of their low micromolar antiplasmodium activities, high selectivity

indices and low resistance indices, both ferrocene-quinoline conjugates **6a** and **7a** can be considered as valuable new hit molecules for elaboration follow-up studies in malaria research.

4. Experimental section

4.1. Chemistry

4.1.1. General

All chemicals were commercially available and used as received, except the solvents, which were purified by distillation.

Chromatographic separations were carried out using silica gel 60 (particle size distribution 40–63 μm) purchased from Merck (Darmstadt, Germany), whereas silica gel plates (Merck Silicagel 60 F_{254}, precoated, layer thickness 0.25 mm) was used for TLC. Proton (^{1}H) and Carbon (^{13}C) NMR spectra were recorded on a Bruker Avance III 400 spectrometer (400 MHz for ^{1}H, 101 MHz for ^{13}C). Solutions were prepared in deuterochloroform ($CDCl_3$) and chemical shifts are expressed in ppm (δ) using tetramethylsilane as the internal standard. 2D experiments (COSY, NOESY, HSQC and HMBC) were run on the Bruker Avance III 400 spectrometer with the usual pulse sequences. HPLC-MS analyses were performed on an Agilent 1200 series HPLC system equipped with a Supelco Ascentis Express C18 column (3 cm × 4.6 mm, 2.7 μm fused-core particles, 90 Å), Phenomex Guard column (SecurityGuard Standard) and a UV-DAD detector. The HPLC is coupled to an Agilent 1100 Series MS with electrospray ionization (70 eV) with a single quadrupole detector.

The IR measurements were carried out in neat form with an ATR (Attenuated Total Reflectance) accessory with a Shimadzu IRAFFINITY-1S WL FTIR spectrophotometer.

The GC/MS analyses were performed on a Hewlett-Packard 6890/5973N gas chromatograph/mass spectrometer equipped with a Phenomex Zebron ZB-5MSplus (30 m × 0.25 mm × 0.25 μm) column and quadrupole mass analyzer (Electron Ionization, 70 eV). Cyclic voltammetry experiments were performed at room temperature in a standard three-electrode cell using an Autolab potentiostat (PGSTAT 302 N). The working electrode was a platinum disk (2 mm diameter; Metrohm). The counter electrode was a platinum wire, whereas an Ag/AgCl electrode was used as the reference. Prior to experiments, the working electrode was polished using Metrohm polishing kit 6.2802.000 (extremely fine aluminum oxide on a cloth), followed by washing with distilled water.

Melting points were measured on a Mel-Temp cap. Melting points apparatus, model 1001, and the given values are uncorrected. Ultrasonic cleaner Elmasonic S 10, 30 W was used for the ultrasonically supported synthesis.

4.1.2. General procedure for the synthesis of 1-ferrocenyl-3-(quinolinylamino)propan-1-ones (**5a-e**)

A solution of the corresponding aminoquinoline (2 mmol) and 1-ferrocenylpropenone **3** [17–20] (1 mmol) in 0.1 M Na_2CO_3 (0.5 mmol, 5 ml) was stirred at reflux conditions overnight (around 15 h). The reaction mixture was quenched by addition of cold water (20 ml) and the products were extracted with CH_2Cl_2 (two 20 ml portions). The organic layer was washed with brine and dried over anh. Na_2SO_4. After evaporation of the solvent, the crude mixture was purified by column chromatography (SiO_2), affording pure products **5a-e**.

*4.1.2.1. 1-Ferrocenyl-3-(quinolin-4-ylamino)propan-1-one (**5a**).* Dark orange solid; mp 162 °C. Rf = 0.38 (EtOAc/MeOH, 9:1 (v/v)). Yield 57%. ^{1}H NMR (400 MHz, $CDCl_3$): δ = 8.60 (d, J = 5.3 Hz, 1H, CH_{Ar}), 7.97 (d, J = 8.3 Hz, 1H, CH_{Ar}), 7.77 (d, J = 8.4 Hz, 1H, CH_{Ar}), 7.62 (ddd, J = 8.4, 7.0, 1.3 Hz, 1H, CH_{Ar}), 7.44 (ddd, J = 8.3, 7.0, 1.1 Hz, 1H, CH_{Ar}), 6.51 (d, J = 5.3 Hz, 1H, CH_{Ar}), 5.84 (t, J = 5.8 Hz, 1H, $CH_2CH_2\underline{N}H$), 4.80 (pseudo t, J = 1.9 Hz, 2H, 2 × CH_{Cp}), 4.54 (pseudo t, J = 1.9 Hz, 2H, 2 × CH_{Cp}), 4.09 (s, 5H, 5 × CH_{Cp}), 3.80 (td, J = 5.9, 5.8 Hz, 2H, $CH_2\underline{C}H_2NH$), 3.15 (t, J = 5.9 Hz, 2H, $\underline{C}H_2CH_2NH$). ^{13}C NMR (101 MHz, $CDCl_3$): δ = 203.4 (C═O), 150.5 (C_{Ar}), 149.6 (C_{Ar}), 148.1 (C_{Ar}), 129.5 (C_{Ar}), 129.3 (C_{Ar}), 124.9 (C_{Ar}), 119.6 (C_{Ar}), 118.9 (C_{Ar}), 98.4 (C_{Ar}), 78.4 (C_{Cp}), 72.8 (2 × C_{Cp}), 69.9 (5 × C_{Cp}), 69.3 (2 × C_{Cp}), 38.1 ($CH_2\underline{C}H_2NH$), 37.5 ($\underline{C}H_2CH_2NH$). IR (ATR, cm^{-1}): ν = 3210 (N–H) cm^{-1}; ν = 1651 (C═O) cm^{-1}. MS (70eV): m/z (%) 385.0 ([M + H]$^+$). HRMS (ESI): m/z for $C_{22}H_{20}FeN_2O$ [M+H]$^+$ calcd 385.0998, found 385.0991.

*4.1.2.2. 1-Ferrocenyl-3-(quinolin-3-ylamino)propan-1-one (**5b**).* Dark orange solid; mp 166 °C. Rf = 0.72 (EtOAc/MeOH, 9:1 (v/v)). Yield 71%. ^{1}H NMR (400 MHz, $CDCl_3$): δ = 8.46 (d, J = 2.8 Hz, 1H, CH_{Ar}), 7.96–7.91 (m, 1H, CH_{Ar}), 7.65–7.62 (m, 1H, CH_{Ar}), 7.46–7.38 (m, 2H, 2 × CH_{Ar}), 7.10 (d, J = 2.8 Hz, 1H, CH_{Ar}), 4.79 (pseudo t, J = 1.9 Hz, 2H, 2 × CH_{Cp}), 4.60 (t, J = 6.2 Hz, 1H, $CH_2CH_2N\underline{H}$), 4.53 (pseudo t, J = 1.9 Hz, 2H, 2 × CH_{Cp}), 4.15 (s, 5H, 5 × CH_{Cp}), 3.67 (td, J = 6.2, 6.2 Hz, 2H, $CH_2\underline{C}H_2NH$), 3.11 (t, J = 6.2 Hz, 2H, $\underline{C}H_2CH_2NH$). ^{13}C NMR (101 MHz, $CDCl_3$): δ 203.3 (C═O), 143.6 (C_{Ar}), 142.2 (C_{Ar}), 141.2 (C_{Ar}), 129.4 (C_{Ar}), 129.1 (C_{Ar}), 127.0 (C_{Ar}), 125.9 (C_{Ar}), 125.0 (C_{Ar}), 110.2 (C_{Ar}), 78.6 (C_{Cp}), 72.7 (2 × C_{Cp}), 69.9 (5 × C_{Cp}), 69.3 (2 × C_{Cp}), 38.6 ($CH_2\underline{C}H_2NH$), 37.9 ($\underline{C}H_2CH_2NH$). IR (ATR, cm^{-1}): ν = 3363 (N–H) cm^{-1}; ν = 1645 (C═O) cm^{-1}. MS (70eV): m/z (%) 385.0 ([M + H]$^+$). HRMS (ESI): m/z for $C_{22}H_{20}FeN_2O$ [M+H]$^+$ calcd 385.0998, found 385.1011.

*4.1.2.3. 1-Ferrocenyl-3-(quinolin-5-ylamino)propan-1-one (**5c**).* Dark orange solid; mp 125 °C. Rf = 0.82 (EtOAc/MeOH, 9:1 (v/v)). Yield 90%. ^{1}H NMR (400 MHz, $CDCl_3$): δ = 8.85 (dd, J = 4.1, 1.3 Hz, 1H, CH_{Ar}), 8.21 (d, J = 8.6 Hz, 1H, CH_{Ar}), 7.59 (dd, J = 8.4, 7.7 Hz, 1H, CH_{Ar}), 7.49 (d, J = 8.4 Hz, 1H, CH_{Ar}), 7.32 (dd, J = 8.6, 4.1 Hz, 1H, CH_{Ar}), 6.71 (d, J = 7.7 Hz, 1H, CH_{Ar}), 5.24 (br s, 1H, $CH_2CH_2N\underline{H}$), 4.79 (pseudo t, J = 1.9 Hz, 2H, 2 × CH_{Cp}), 4.52 (pseudo t, J = 1.9 Hz, 2H, 2 × CH_{Cp}), 4.09 (s, 5H, 5 × CH_{Cp}), 3.73 (t, J = 5.8 Hz, 2H, $CH_2\underline{C}H_2NH$), 3.15 (t, J = 5.8 Hz, 2H, $\underline{C}H_2CH_2NH$). ^{13}C NMR (100 MHz, $CDCl_3$): δ = 204.0 (C═O), 150.1 (C_{Ar}), 149.3 (C_{Ar}), 143.4 (C_{Ar}), 130.3 (C_{Ar}), 129.0 (C_{Ar}), 119.6 (C_{Ar}), 118.8 (C_{Ar}), 118.6 (C_{Ar}), 104.5 (C_{Ar}), 78.6 (C_{Cp}), 72.7 (2 × C_{Cp}), 69.9 (5 × C_{Cp}), 69.3 (2 × C_{Cp}), 39.2 ($CH_2\underline{C}H_2NH$), 37.7 ($\underline{C}H_2CH_2NH$). IR (ATR, cm^{-1}): ν = 3293 (N–H) cm^{-1}; ν = 1659 (C═O) cm^{-1}. MS (70eV): m/z (%) 385.0 ([M + H]$^+$).

*4.1.2.4. 1-Ferrocenyl-3-(quinolin-6-ylamino)propan-1-one (**5d**).* Dark orange solid; mp 130 °C. Rf = 0.85 (EtOAc/MeOH, 9:1 (v/v)). Yield 87%. ^{1}H NMR (400 MHz, $CDCl_3$): δ = 8.61 (dd, J = 4.1, 1.2 Hz, 1H, CH_{Ar}), 7.93 (d, J = 8.3 Hz, 1H, CH_{Ar}), 7.87 (d, J = 9.0 Hz, 1H, CH_{Ar}), 7.26 (dd, J = 8.3, 4.1 Hz, 1H, CH_{Ar}), 7.11 (dd, J = 9.0, 2.4 Hz, 1H, CH_{Ar}), 6.78 (d, J = 2.4 Hz, 1H, CH_{Ar}), 4.78 (pseudo t, J = 1.7 Hz, 2H, 2 × CH_{Cp}), 4.57 (t, J = 5.6 Hz, 1H, $CH_2CH_2N\underline{H}$), 4.52 (pseudo t, J = 1.7 Hz, 2H, 2 × CH_{Cp}), 4.12 (s, 5H, 5 × CH_{Cp}), 3.68 (td, J = 5.7, 5.6 Hz, 2H, $CH_2\underline{C}H_2NH$), 3.10 (t, J = 5.7 Hz, 2H, $\underline{C}H_2CH_2NH$). ^{13}C NMR (100 MHz, $CDCl_3$): δ = 203.4 (C═O), 146.2 (C_{Ar}), 145.7 (C_{Ar}), 143.3 (C_{Ar}), 133.8 (C_{Ar}), 130.5 (C_{Ar}), 130.1 (C_{Ar}), 121.6 (C_{Ar}), 121.4 (C_{Ar}), 103.0 (C_{Ar}), 78.7 (C_{Cp}), 72.6 (2 × C_{Cp}), 69.9 (5 × C_{Cp}), 69.3 (2 × C_{Cp}), 38.8 ($CH_2\underline{C}H_2NH$), 38.0 ($\underline{C}H_2CH_2NH$). IR (ATR, cm^{-1}): ν = 3329 (N–H) cm^{-1}; ν = 1658 (C═O) cm^{-1}. MS (70eV): m/z (%) 385.0 ([M + H]$^+$).

*4.1.2.5. 1-Ferrocenyl-3-(quinolin-8-ylamino)propan-1-one (**5e**).* Dark orange solid; mp 127 °C. Rf = 0.48 (Toluene/EtOAc, 9:1 (v/v)). Yield 91%. ^{1}H NMR (400 MHz, $CDCl_3$): δ = 8.71 (dd, J = 4.2, 1.8 Hz, 1H, CH_{Ar}), 8.04 (dd, J = 8.3, 1.8 Hz, 1H, CH_{Ar}), 7.42 (dd, J = 8.0, 7.8 Hz, 1H, CH_{Ar}), 7.35 (dd, J = 8.3, 4.2 Hz, 1H, CH_{Ar}), 7.06 (dd, J = 8.0, 0.9 Hz, 1H, CH_{Ar}), 6.78 (dd, J = 7.8, 0.9 Hz, 1H, CH_{Ar}), 6.42 (t, J = 6.3 Hz, 1H, $CH_2CH_2N\underline{H}$), 4.80 (pseudo t, J = 1.9 Hz, 2H, 2 × CH_{Cp}), 4.50 (pseudo t,

J = 1.9 Hz, 2H, 2 × CH_{Cp}), 4.12 (s, 5H, 5 × CH_{Cp}), 3.81 (td, J = 6.6, 6.3 Hz, 2H, $CH_2\underline{CH_2}NH$), 3.17 (t, J = 6.6 Hz, 2H, $\underline{CH_2}CH_2NH$). ^{13}C NMR (100 MHz, $CDCl_3$): δ = 202.8 (C═O), 147.0 (C_{Ar}), 144.4 (C_{Ar}), 138.4 (C_{Ar}), 136.0 (C_{Ar}), 128.7 (C_{Ar}), 127.7 (C_{Ar}), 121.5 (C_{Ar}), 114.0 (C_{Ar}), 104.5 (C_{Ar}), 79.0 (C_{Cp}), 72.4 (2 × C_{Cp}), 69.8 (5 × C_{Cp}), 69.3 (2 × C_{Cp}), 38.7 ($CH_2\underline{CH_2}NH$), 38.1 ($\underline{CH_2}CH_2NH$). IR (ATR, cm^{-1}): ν = 3400 (N–H) cm^{-1}; ν = 1664 (C═O) cm^{-1}. MS (70eV): m/z (%) 385.0 ([M+ H]$^+$).

4.1.3. General procedure for the synthesis of 1-ferrocenyl-3-(quinolinylamino)propan-1-ols (**6a-e**)

To a stirred solution of the corresponding 1-ferrocenyl-3-(quinolinylamino)propan-1-one **5a-e** (1 mmol) in MeOH (20 ml) at room temperature, an excess of $NaBH_4$ (5 mmol) was added in several portions (up to 190 mg) and the reaction progress was monitored by TLC. After completion of the reduction (*ca*. 2 h), methanol was distilled off and the residue was diluted with water (20 ml). The mixture was extracted with CH_2Cl_2 (two 20 ml portions) and the collected organic layers were washed with water and brine and dried with anh. Na_2SO_4. After filtering off the drying agent and evaporation of the solvent, the crude mixture was purified by column chromatography (SiO_2), affording pure products **6a-e**.

4.1.3.1. 1-Ferrocenyl-3-(quinolin-4-ylamino)propan-1-ol (**6a**).

Yellow solid; mp 172 °C. Rf = 0.47 (EtOAc/MeOH, 9:1 (v/v)). Yield 91%. ^{1}H NMR (400 MHz, $CDCl_3$) δ = 8.53 (d, J = 5.3 Hz, 1H, CH_{Ar}), 7.98 (dd, J = 8.4, 1.0 Hz, 1H, CH_{Ar}), 7.73 (dd, J = 8.4, 1.0 Hz, 1H, CH_{Ar}), 7.62 (ddd, J = 8.4, 7.0, 1.0 Hz, 1H, CH_{Ar}), 7.42 (ddd, J = 8.4, 7.0, 1.0 Hz, 1H, CH_{Ar}), 6.37 (d, J = 5.3 Hz, 1H, CH_{Ar}), 6.11 (br s, 1H, $CHCH_2CH_2N\underline{H}$), 4.66 (dd, J = 8.3, 3.4 Hz, 1H, $C\underline{H}OH$), 4.29–4.27 (m, 1H, CH_{Cp}), 4.24–4.20 (m, 8H, 8 × CH_{Cp}), 3.53–3.39 (m, 2H, $CHCH_2C\underline{H_2}NH$), 2.26–2.15 (m, 3H, CHO$\underline{H}$ and $CHC\underline{H_2}CH_2NH$). ^{13}C NMR (101 MHz, $CDCl_3$) δ = 150.8 (C_{Ar}), 150.1 (C_{Ar}), 148.0 (C_{Ar}), 129.5 (C_{Ar}), 129.1 (C_{Ar}), 124.6 (C_{Ar}), 119.7 (C_{Ar}), 118.8 (C_{Ar}), 98.3 (C_{Ar}), 93.3 (C_{Cp}), 69.9 (CHOH), 68.4 (5 × C_{Cp}), 68.33 (C_{Cp}), 68.30 (C_{Cp}), 67.0 (C_{Cp}), 65.2 (C_{Cp}), 41.3 ($CHCH_2\underline{CH_2}NH$), 36.0 ($CH\underline{CH_2}CH_2NH$). IR (ATR, cm^{-1}): ν = 3280 (N–H) cm^{-1}; ν = 3080 (O–H) cm^{-1}. MS (70eV): m/z (%) 387.0 ([M+ H]$^+$). HRMS (ESI): m/z for $C_{22}H_{22}FeN_2O$ [M+H]$^+$ calcd 387.1155, found 387.1163.

4.1.3.2. 1-Ferrocenyl-3-(quinolin-3-ylamino)propan-1-ol (**6b**).

Yellow solid; mp 146 °C. Rf = 0.82 (EtOAc/MeOH, 9:1 (v/v)). Yield 86%. ^{1}H NMR (400 MHz, $CDCl_3$): δ = 8.41 (d, J = 2.8 Hz, 1H, CH_{Ar}), 7.95–7.91 (m, 1H, CH_{Ar}), 7.62–7.58 (m, 1H, CH_{Ar}), 7.44–7.36 (m, 2H, 2 × CH_{Ar}), 6.99 (d, J = 2.8 Hz, 1H, CH_{Ar}), 4.58 (dd, J = 8.2, 4.1 Hz, 1H, $C\underline{H}OH$), 4.48 (t, J = 4.9 Hz, 1H, $CHCH_2CH_2N\underline{H}$), 4.28–4.26 (m, 1H, $C\underline{H}_{Cp}$), 4.23–4.19 (m, 8H, 8 × CH_{Cp}), 3.39–3.35 (m, 2H, $CHCH_2C\underline{H_2}NH$), 2.25 (br s, 1H, CHO$\underline{H}$), 2.14–1.97 (m, 2H, $CHC\underline{H_2}CH_2NH$). ^{13}C NMR (101 MHz, $CDCl_3$) δ = 143.7 (C_{Ar}), 142.0 (C_{Ar}), 141.7 (C_{Ar}), 129.6 (C_{Ar}), 129.0 (C_{Ar}), 126.9 (C_{Ar}), 125.9 (C_{Ar}), 124.7 (C_{Ar}), 109.8 (C_{Ar}), 93.6 (C_{Cp}), 68.9 (CHOH), 68.4 (5 × C_{Cp}), 68.3 (C_{Cp}), 68.2 (C_{Cp}), 67.0 (C_{Cp}), 65.2 (C_{Cp}), 41.2 ($CHCH_2\underline{CH_2}NH$), 36.6 ($CH\underline{CH_2}CH_2NH$). IR (ATR, cm^{-1}): ν = 3300 (N–H) cm^{-1}; ν = 3200 (O–H) cm^{-1}. MS (70eV): m/z (%) 387.0 ([M+ H]$^+$).

4.1.3.3. 1-Ferrocenyl-3-(quinolin-5-ylamino)propan-1-ol (**6c**).

Yellow solid; mp 169 °C. Rf = 0.85 (EtOAc/MeOH, 9:1 (v/v)). Yield 98%. ^{1}H NMR (400 MHz, $CDCl_3$) δ = 8.85 (dd, J = 4.2, 1.4 Hz, 1H, CH_{Ar}), 8.14 (d, J = 8.5 Hz, 1H, CH_{Ar}), 7.55 (dd, J = 8.2, 7.8 Hz, 1H, CH_{Ar}), 7.45 (d, J = 8.2 Hz, 1H, CH_{Ar}), 7.30 (dd, J = 8.5, 4.2 Hz, 1H, CH_{Ar}), 6.59 (d, J = 7.8 Hz, 1H, CH_{Ar}), 5.24 (s, 1H, $CHCH_2CH_2N\underline{H}$), 4.64 (dd, J = 8.2, 3.8 Hz, 1H, $C\underline{H}OH$), 4.29–4.27 (m, 1H, CH_{Cp}), 4.24–4.18 (m, 8H, 8 × CH_{Cp}), 3.50–3.35 (m, 2H, $CHCH_2C\underline{H_2}NH$), 2.46 (br s, 1H, CHO$\underline{H}$), 2.23–2.07 (m, 2H, $CHC\underline{H_2}CH_2NH$). ^{13}C NMR (101 MHz, $CDCl_3$) δ = 149.9 (C_{Ar}), 149.2 (C_{Ar}), 144.1 (C_{Ar}), 130.5 (C_{Ar}), 129.1 (C_{Ar}), 119.2 (C_{Ar}), 118.5 (C_{Ar}), 117.9 (C_{Ar}), 104.1 (C_{Ar}), 93.6 (C_{Cp}), 69.9 (CHOH), 68.4 (5 × C_{Cp}), 68.3 (C_{Cp}), 68.2 (C_{Cp}), 67.0 (C_{Cp}), 65.3 (C_{Cp}), 42.2 ($CHCH_2\underline{CH_2}NH$), 36.5 ($CH\underline{CH_2}CH_2NH$). IR (ATR, cm^{-1}): ν = 3420 (N–H) cm^{-1}; ν = 3363 (O–H) cm^{-1}. MS (70eV): m/z (%) 387.0 ([M+ H]$^+$). HRMS (ESI): m/z for $C_{22}H_{22}FeN_2O$ [M+H]$^+$ calcd 387.1155, found 387.1162.

4.1.3.4. 1-Ferrocenyl-3-(quinolin-6-ylamino)propan-1-ol (**6d**).

Yellow solid; mp 131 °C. Rf = 0.32 (EtOAc/MeOH, 9:1 (v/v)). Yield 97%. ^{1}H NMR (400 MHz, $CDCl_3$) δ = 8.60 (dd, J = 4.1, 1.4 Hz, 1H, CH_{Ar}), 7.90 (dd, J = 8.2, 1.4 Hz, 1H, CH_{Ar}), 7.86 (d, J = 9.0 Hz, 1H, CH_{Ar}), 7.25 (dd, J = 8.2, 4.1 Hz, 1H, CH_{Ar}), 7.08 (dd, J = 9.0, 2.6 Hz, 1H, CH_{Ar}), 6.68 (d, J = 2.6 Hz, 1H, CH_{Ar}), 4.57 (dd, J = 8.2, 4.2 Hz, 1H, $C\underline{H}OH$), 4.42 (br s, 1H, $CHCH_2CH_2N\underline{H}$), 4.27–4.26 (m, 1H, CH_{Cp}), 4.22–4.18 (m, 8H, 8 × CH_{Cp}), 3.38 (t, J = 6.4 Hz, 2H, $CHCH_2C\underline{H_2}NH$), 2.25 (br s, 1H, CHO$\underline{H}$), 2.13–1.97 (m, 2H, $CHC\underline{H_2}CH_2NH$). ^{13}C NMR (101 MHz, $CDCl_3$) δ = 146.3 (C_{Ar}), 146.0 (C_{Ar}), 143.2 (C_{Ar}), 133.8 (C_{Ar}), 130.20 (C_{Ar}), 130.17 (C_{Ar}), 121.6 (C_{Ar}), 121.3 (C_{Ar}), 102.8 (C_{Ar}), 93.6 (C_{Cp}), 68.9 (CHOH), 68.4 (5 × C_{Cp}), 68.2 (C_{Cp}), 68.1 (C_{Cp}), 67.0 (C_{Cp}), 65.3 (C_{Cp}), 41.4 ($CHCH_2\underline{CH_2}NH$), 36.8 ($CH\underline{CH_2}CH_2NH$). IR (ATR, cm^{-1}): ν = 3404 (N–H) cm^{-1}; ν = 3212 (O–H) cm^{-1}. MS (70eV): m/z (%) 387.0 ([M+ H]$^+$).

4.1.3.5. 1-Ferrocenyl-3-(quinolin-8-ylamino)propan-1-ol (**6e**).

Yellow solid; mp 98 °C. Rf = 0.48 (Toluene/EtOAc, 9:1 (v/v)). Yield 95%. ^{1}H NMR (400 MHz, $CDCl_3$) δ = 8.71 (dd, J = 4.2, 1.7 Hz, 1H, CH_{Ar}), 8.04 (dd, J = 8.3, 1.7 Hz, 1H, CH_{Ar}), 7.37 (dd, J = 8.0, 7.8 Hz, 1H, CH_{Ar}), 7.35 (dd, J = 8.3, 4.2 Hz, 1H, CH_{Ar}), 7.03 (dd, J = 8.0, 0.8 Hz, 1H, CH_{Ar}), 6.69 (dd, J = 7.8, 0.8 Hz, 1H, CH_{Ar}), 6.33 (br s, 1H, $CHCH_2CH_2N\underline{H}$), 4.59 (dd, J = 8.1, 4.1 Hz, 1H, $C\underline{H}OH$), 4.27–4.26 (m, 1H, CH_{Cp}), 4.21–4.20 (m, 1H, CH_{Cp}), 4.18–4.15 (m, 7H, 7 × CH_{Cp}), 3.48 (t, J = 6.6 Hz, 2H, $CHCH_2C\underline{H_2}NH$), 2.21–2.05 (m, 3H, CHO$\underline{H}$ and $CHC\underline{H_2}CH_2NH$). ^{13}C NMR (101 MHz, $CDCl_3$) δ = 146.9 (C_{Ar}), 144.9 (C_{Ar}), 138.3 (C_{Ar}), 136.0 (C_{Ar}), 128.7 (C_{Ar}), 127.9 (C_{Ar}), 121.4 (C_{Ar}), 113.8 (C_{Ar}), 104.7 (C_{Ar}), 93.8 (C_{Cp}), 68.4 (5 × C_{Cp}), 68.2 (CHOH), 68.1 (C_{Cp}), 68.0 (C_{Cp}), 67.0 (C_{Cp}), 65.6 (C_{Cp}), 40.7 ($CHCH_2\underline{CH_2}NH$), 37.3 ($CH\underline{CH_2}CH_2NH$). IR (ATR, cm^{-1}): ν = 3410 (N–H) cm^{-1}; ν = 3302 (O–H) cm^{-1}. MS (70eV): m/z (%) 387.0 ([M+ H]$^+$).

4.1.4. General procedure for the synthesis of N-(3-ferrocenylprop-2-en-1-yl)-2,2,2-trifluoro-N-(quinolinyl)acetamides (**7a-e**)

Triethylamine (1.5 mmol) and trifluoroacetic anhydride (1.5 mmol) were added dropwise to a cooled solution (an ice bath) of the corresponding 1,3-aminoalcohol **6a-e** (1 mmol) in 5 ml of dry tetrahydrofuran (THF). The reaction mixture was stirred for 16 h (first 5 h in an ice bath) under nitrogen atmosphere. After that, THF was evaporated, the mixture was neutralized with a saturated solution of $NaHCO_3$ (litmus paper) and extracted with CH_2Cl_2 (two 20 ml portions). The combined organic layers were washed with water, brine and dried over anh. Na_2SO_4. After filtration, the solvent was evaporated, and the crude product **7a-e** was purified by column chromatography (SiO_2).

4.1.4.1. (E)-N-(3-Ferrocenylprop-2-en-1-yl)-2,2,2-trifluoro-N-(quinolin-4-yl)acetamide (**7a**).

Dark red oil; Rf = 0.67 (Petroleum ether/EtOAc, 7:3 (v/v)). Yield 80%. ^{1}H NMR (400 MHz, $CDCl_3$) δ = 8.99 (d, J = 4.5 Hz, 1H, CH_{Ar}), 8.24 (d, J = 8.5 Hz, 1H, CH_{Ar}), 7.88–7.81 (m, 2H, 2 × CH_{Ar}), 7.70 (ddd, J = 8.8, 7.0, 1.0 Hz, 1H, CH_{Ar}), 7.24 (d, J = 4.5 Hz, 1H, CH_{Ar}), 6.14 (d, J = 15.5 Hz, 1H, $C\underline{H}$═$CHCH_2$), 5.83 (ddd, J = 15.5, 8.4, 6.2 Hz, 1H, CH═$C\underline{H}CH_2$), 4.97 (ddd, J = 14.0, 6.2, 0.9 Hz, 1H, CH═CH($\underline{H}$CH)), 4.28–4.18 (m, 4H, 4 × CH_{Cp}), 3.99 (s, 5H, 5 × CH_{Cp}),

3.92 (dd, J = 14.0, 8.4 Hz, 1H, CH=CH(HCH)). ^{13}C NMR (101 MHz, $CDCl_3$) δ = 156.5 (NC=OCF_3)*, 150.3 (C_{Ar}), 149.9 (C_{Ar}), 143.1 (C_{Ar}), 134.9 (CH=$CHCH_2$), 130.5 (C_{Ar}), 130.4 (C_{Ar}), 128.3 (C_{Ar}), 125.2 (C_{Ar}), 122.2 (C_{Ar}), 121.4 (C_{Ar}), 117.6 (CH=$CHCH_2$), 114.6 (CF_3)*, 81.3 (C_{Cp}), 69.2 (2 × C_{Cp}), 69.1 (5 × C_{Cp}), 67.2 (C_{Cp}), 66.8 (C_{Cp}), 53.8 (CH_2). ^{19}F NMR (376 MHz, $CDCl_3$) δ = −75.6 (CF_3). IR (ATR, cm^{-1}): ν = 1697 (C=O) cm^{-1}. MS (70eV): m/z (%) 465.0 ([M+ H]$^+$).

*4.1.4.2. (E)-N-(3-Ferrocenylprop-2-en-1-yl)-2,2,2-trifluoro-N-(quinolin-3-yl)acetamide (**7b**).* Dark red solid; mp 88 °C. Rf = 0.62 (Petroleum ether/EtOAc, 9:1 (v/v)). Yield 84%. ^{1}H NMR (400 MHz, $CDCl_3$) δ = 8.80 (d, J = 2.0 Hz, 1H, CH_{Ar}), 8.17 (d, J = 8.4 Hz, 1H, CH_{Ar}), 8.03 (d, J = 2.0 Hz, 1H, CH_{Ar}), 7.87 (d, J = 8.2 Hz, 1H, CH_{Ar}), 7.81 (ddd, J = 8.4, 7.0, 1.3 Hz, 1H, CH_{Ar}), 7.63 (ddd, J = 8.2, 7.0, 1.1 Hz, 1H, CH_{Ar}), 6.20 (d, J = 15.5 Hz, 1H, CH=$CHCH_2$), 5.82 (ddd, J = 15.5, 7.1, 7.1 Hz, 1H, CH=$CHCH_2$), 4.46 (d, J = 7.1 Hz, 2H, CH=$CHCH_2$), 4.27–4.25 (m, 2H, 2 × CH_{Cp}), 4.21–4.20 (m, 2H, 2 × CH_{Cp}), 3.98 (s, 5H, 5 × CH_{Cp}). ^{13}C NMR (101 MHz, $CDCl_3$) δ = 156.7 (q, J = 36.0 Hz, NC=OCF_3), 150.0 (C_{Ar}), 147.6 (C_{Ar}), 135.2 (C_{Ar}), 134.7 (CH=$CHCH_2$), 132.2 (C_{Ar}), 130.9 (C_{Ar}), 129.6 (C_{Ar}), 128.1 (C_{Ar}), 127.9 (C_{Ar}), 127.2 (C_{Ar}), 117.7 (CH=$CHCH_2$), 116.2 (q, J = 288.5 Hz, CF_3), 81.4 (C_{Cp}), 69.12 (2 × C_{Cp}), 69.1 (5 × C_{Cp}), 67.0 (2 × C_{Cp}), 54.5 (C, CH_2). ^{19}F NMR (376 MHz, $CDCl_3$) δ = −67.1 (CF_3). IR (ATR, cm^{-1}): ν = 1693 (C=O) cm^{-1}. MS (70eV): m/z (%) 465.0 ([M+ H]$^+$). HRMS (ESI): m/z for $C_{24}H_{19}F_3FeN_2O$ [M+H]$^+$ calcd 465.0872, found 465.0887.

*4.1.4.3. (E)-N-(3-Ferrocenylprop-2-en-1-yl)-2,2,2-trifluoro-N-(quinolin-5-yl)acetamide (**7c**).* Dark red oil; Rf = 0.62 (Petroleum ether/EtOAc, 7:3 (v/v)). Yield 78%. ^{1}H NMR (400 MHz, $CDCl_3$) δ = 9.03 (d, J = 3.9 Hz, 1H, CH_{Ar}), 8.22 (d, J = 8.6 Hz, 1H, CH_{Ar}), 8.18 (d, J = 8.4 Hz, 1H, CH_{Ar}), 7.75 (dd, J = 8.4, 7.4 Hz, 1H, CH_{Ar}), 7.55 (dd, J = 8.6, 3.9 Hz, 1H, CH_{Ar}), 7.43 (d, J = 7.4 Hz, 1H, CH_{Ar}), 6.12 (d, J = 15.5 Hz, 1H, CH=$CHCH_2$), 5.84 (ddd, J = 15.5, 8.2, 6.3 Hz, 1H, CH=$CHCH_2$), 4.92 (ddd, J = 13.9, 6.3, 0.9 Hz, 1H, CH=CH(HCH)), 4.30–4.20 (m, 4H, 4 × CH_{Cp}), 4.01 (s, 5H, 5 × CH_{Cp}), 3.91 (dd, J = 13.9, 8.2 Hz, 1H, CH, CH=CH(HCH)). ^{13}C NMR (101 MHz, $CDCl_3$) δ = 157.4 (q, J = 36.1 Hz, NC=OCF_3), 156.5 (C_{Ar}), 151.2 (C_{Ar}), 148.9 (C_{Ar}), 134.6 (CH=$CHCH_2$), 131.5 (C_{Ar}), 130.8 (C_{Ar}), 128.5 (C_{Ar}), 127.9 (C_{Ar}), 125.7 (C_{Ar}), 122.4 (C_{Ar}), 118.1 (CH=$CHCH_2$), 116.2 (q, J = 288.6 Hz, CF_3), 81.6 (C_{Cp}), 69.22 (5 × C_{Cp}), 69.20 (2 × C_{Cp}), 67.04 (C_{Cp}), 67.00 (C_{Cp}), 53.4 (CH_2). ^{19}F NMR (376 MHz, $CDCl_3$) δ = −68.3 (CF_3). IR (ATR, cm^{-1}): ν = 1593 (C=O) cm^{-1}. MS (70eV): m/z (%) 465.0 ([M+ H]$^+$).

*4.1.4.4. (E)-N-(3-Ferrocenylprop-2-en-1-yl)-2,2,2-trifluoro-N-(quinolin-6-yl)acetamide (**7d**).* Dark red solid; mp = 83 °C. Rf = 0.71 (Petroleum ether/EtOAc, 7:3 (v/v)). Yield 87%. ^{1}H NMR (400 MHz, $CDCl_3$) δ = 8.99 (d, J = 3.9 Hz, 1H, CH_{Ar}), 8.20 (d, J = 8.7 Hz, 1H, CH_{Ar}), 8.18 (d, J = 8.1 Hz, 1H, CH_{Ar}), 7.69 (s, 1H, CH_{Ar}), 7.57 (dd, J = 8.7, 1.7 Hz, 1H, CH_{Ar}), 7.47 (dd, J = 8.1, 3.9 Hz, 1H, CH_{Ar}), 6.20 (d, J = 15.6 Hz, 1H, CH=$CHCH_2$), 5.88–5.81 (m, 1H, CH=$CHCH_2$), 4.50–4.38 (m, 2H, CH=$CHCH_2$), 4.29–4.26 (m, 2H, 2 × CH_{Cp}), 4.22–4.19 (m, 2H, 2 × CH_{Cp}), 3.99 (s, 5H, 5 × CH_{Cp}). ^{13}C NMR (101 MHz, $CDCl_3$) δ = 156.6 (q, J = 35.6 Hz, NC=OCF_3), 151.8 (C_{Ar}), 147.7 (C_{Ar}), 136.8 (C_{Ar}), 136.3 (C_{Ar}), 134.0 (CH=$CHCH_2$), 131.3 (C_{Ar}), 129.5 (C_{Ar}), 128.0 (C_{Ar}), 127.5 (C_{Ar}), 122.1 (C_{Ar}), 118.3 (CH=$CHCH_2$), 114.9 (q, J = 288.5 Hz, CF_3), 81.5 (C_{Cp}), 69.08 (5 × C_{Cp}), 69.06 (C_{Cp}), 67.0 (2 × Cp), 54.4 (CH_2). ^{19}F NMR (376 MHz, $CDCl_3$) δ = −67.1 (CF_3). IR (ATR, cm^{-1}): ν = 1693 (C=O) cm^{-1}. MS (70eV): m/z (%) 465.0 ([M+ H]$^+$). HRMS (ESI): m/z for $C_{24}H_{19}F_3FeN_2O$ [M+H]$^+$ calcd 465.0872, found 465.0876.

* Coupling between C and F not visible.

*4.1.4.5. (E)-N-(3-Ferrocenylprop-2-en-1-yl)-2,2,2-trifluoro-N-(quinolin-8-yl)acetamide (**7e**).* Dark red oil; Rf = 0.81 (Petroleum ether/EtOAc, 7:3 (v/v)). Yield 81%. ^{1}H NMR (400 MHz, $CDCl_3$) δ = 9.03 (dd, J = 4.2, 1.7 Hz, 1H, CH_{Ar}), 8.25 (dd, J = 8.3, 1.7 Hz, 1H, CH_{Ar}), 7.92 (dd, J = 7.7, 1.9 Hz, 1H, CH_{Ar}), 7.64–7.56 (m, 2H, 2 × CH_{Ar}), 7.53 (dd, J = 8.3, 4.2 Hz, 1H, CH_{Ar}), 6.07 (d, J = 15.6 Hz, 1H, CH=$CHCH_2$), 5.87 (ddd, J = 15.6, 7.7, 6.0 Hz, 1H, CH=$CHCH_2$), 5.06 (dd, J = 14.1, 6.0 Hz, 1H, CH=CH(HCH)), 4.25–4.15 (m, 5H, CH=CH(HCH) and 4 × CH_{Cp}), 3.92 (s, 5H, 5 × CH_{Cp}). ^{13}C NMR (101 MHz, $CDCl_3$) δ = 157.6 (q, J = 35.5 Hz, NC=OCF_3), 151.1 (C_{Ar}), 144.5 (C_{Ar}), 136.3 (C_{Ar}), 136.1 (C_{Ar}), 132.9 (CH=$CHCH_2$), 130.0 (C_{Ar}), 129.5 (C_{Ar}), 129.1 (C_{Ar}), 125.8 (C_{Ar}), 122.1 (C_{Ar}), 119.6 (CH=$CHCH_2$), 116.4 (q, J = 288.6 Hz, CF_3), 81.9 (C_{Cp}), 69.1 (5 × C_{Cp}), 68.8 (2 × C_{Cp}), 66.9 (C_{Cp}), 66.8 (C_{Cp}), 53.6 (CH_2). ^{19}F NMR (376 MHz, $CDCl_3$) δ = −68.4 (CF_3). IR (ATR, cm^{-1}): ν = 1689 (C=O) cm^{-1}. MS (70eV): m/z (%) 465.0 ([M+ H]$^+$).

*4.1.5. General procedure for the synthesis of ferrocene-containing heterotricycles (**8a-e**) [21]*

A mixture of the corresponding ferrocene-containing 1,3-amino alcohol **6a-e** (1 mmol) and glacial acetic acid (0.5 ml) was ultrasonicated in an ultrasonic cleaner for 2 h. The reaction mixture was neutralized with $NaHCO_3$ (litmus paper) and extracted with CH_2Cl_2 (two 20 ml portions). The combined organic layers were washed with water and dried over anh. Na_2SO_4. After filtration, the solvent was evaporated and the crude product (**8a-e**) was purified by column chromatography (SiO_2).

*4.1.5.1. 4-Ferrocenyl-1,2,3,4-tetrahydrobenzo[h] [1,6]naphthyridine (**8a**).* No analytically pure sample could be obtained for compound **8a**. Due to the presence of impurities, no accurate ^{1}H and ^{13}C NMR assignments could thus be provided for this structure.

Yellow solid; mp 196 °C. Rf = 0.48 (EtOAc/MeOH, 9:1 (v/v)). Yield 85%. IR (ATR, cm^{-1}): ν = 2852 (N–H) cm^{-1}. MS (70eV): m/z (%) 369.0 ([M+ H]$^+$).

*4.1.5.2. 1-Ferrocenyl-1,2,3,4-tetrahydrobenzo[f] [1,7]naphthyridine (**8b**).* Yellow solid; mp 203 °C. Rf = 0.34 (Petroleum ether/EtOAc, 7:3 (v/v)). Yield 95%. ^{1}H NMR (400 MHz, $CDCl_3$) δ = 8.31 (s, 1H, CH_{Ar}), 8.07 (d, J = 8.4, 1.2 Hz, 1H, CH_{Ar}), 7.94 (dd, J = 8.3, 1.2 Hz, 1H, CH_{Ar}), 7.50 (ddd, J = 8.4, 6.9, 1.2 Hz, 1H, CH_{Ar}), 7.39 (ddd, J = 8.3, 6.9, 1.2 Hz, 1H, CH_{Ar}), 4.53 (s, 1H, $CHCH_2CH_2NH$), 4.17 (s, 1H, $CHCH_2CH_2NH$), 4.12–4.10 (m, 1H, CH_{Cp}), 4.10–4.07 (m, 6H, 6 × CH_{Cp}), 4.03–4.01 (m, 1H, CH_{Cp}), 3.80–3.77 (m, 1H, CH_{Cp}), 3.46–3.33 (m, 2H, $CHCH_2CH_2NH$), 2.30–2.25 (m, 1H, CH(HCH) CH_2NH), 2.05–1.96 (m, 1H, CH(HCH)CH_2NH). ^{13}C NMR (101 MHz, $CDCl_3$) δ = 142.9 (C_{Ar}), 142.1 (C_{Ar}), 136.6 (C_{Ar}), 129.8 (C_{Ar}), 128.1 (C_{Ar}), 126.3 (C_{Ar}), 124.1 (C_{Ar}), 122.4 (C_{Ar}), 121.0 (C_{Ar}), 93.9 (C_{Cp}), 69.1 (C_{Cp}), 68.9 (5 × C_{Cp}), 67.3 (C_{Cp}), 66.7 (C_{Cp}), 66.6 (C_{Cp}), 37.1 ($CHCH_2CH_2NH$), 30.1 ($CHCH_2CH_2NH$), 27.3 ($CHCH_2CH_2NH$). IR (ATR, cm^{-1}): ν = 2922 (N–H) cm^{-1}. MS (70eV): m/z (%) 369.0 ([M+ H]$^+$). HRMS (ESI): m/z for $C_{22}H_{20}FeN_2$ [M+H]$^+$ calcd 369.1049, found 369.1047.

*4.1.5.3. 4-Ferrocenyl-1,2,3,4-tetrahydro-1,7-phenanthroline (**8c**).* Yellow solid; mp 200 °C. Rf = 0.71 (EtOAc/MeOH, 9:1 (v/v)). Yield 98%. ^{1}H NMR (400 MHz, $CDCl_3$) δ = 8.83 (dd, J = 4.2, 1.2 Hz, 1H, CH_{Ar}), 8.06 (d, J = 8.5 Hz, 1H, CH_{Ar}), 7.57 (d, J = 8.6 Hz, 1H, CH_{Ar}), 7.43 (d, J = 8.6 Hz, 1H, CH_{Ar}), 7.29 (dd, J = 8.5, 4.2 Hz, 1H, CH_{Ar}), 4.53 (s, 1H, $CHCH_2CH_2NH$), 4.19 (s, 5H, 5 × CH_{Cp}), 4.16–4.13 (m, 2H, 2 × CH_{Cp}), 4.08–4.05 (m, 1H, CH_{Cp}), 4.03 (t, J = 4.8 Hz, 1H, $CHCH_2CH_2NH$), 3.79 (s, 1H, CH_{Cp}), 3.47–3.40 (m, 1H, $CHCH_2$(HCH) NH), 3.37–3.28 (m, 1H, $CHCH_2$(HCH)NH), 2.25–2.24 (m, 1H, CH(HCH)CH_2NH), 2.11–2.04 (m, 1H, CH(HCH)CH_2NH). ^{13}C NMR (101 MHz, $CDCl_3$) δ = 149.5 (C_{Ar}), 148.3 (C_{Ar}), 138.6 (C_{Ar}), 132.4 (C_{Ar}), 128.5 (C_{Ar}), 119.2 (C_{Ar}), 118.0 (C_{Ar}), 117.8 (C_{Ar}), 117.1 (C_{Ar}), 94.3 (C_{Cp}), 69.8 (C_{Cp}), 68.8 (5 × C_{Cp}), 67.9 (C_{Cp}), 66.7 (C_{Cp}), 65.8 (C_{Cp}), 39.0

(CHCH$_2$CH$_2$NH), 36.4 (CHCH$_2$CH$_2$NH), 29.5 (CHCH$_2$CH$_2$NH). IR (ATR, cm^{-1}): ν = 2916 (N–H) cm^{-1}. MS (70eV): *m/z* (%) 369.0 ([M+ H]$^+$).

*4.1.5.4. 1-Ferrocenyl-1,2,3,4-tetrahydro-4,7-phenanthroline (**8d**).* Yellow solid; mp 180 °C. Rf = 0.83 (EtOAc/MeOH, 9:1 (v/v)). Yield 95%. ^{1}H NMR (400 MHz, CDCl$_3$) δ = 8.60 (dd, J = 4.2, 1.4 Hz, 1H, CH$_{Ar}$), 8.40 (d, J = 8.5 Hz, 1H, CH$_{Ar}$), 7.77 (d, J = 9.0 Hz, 1H, CH$_{Ar}$), 7.34 (dd, J = 8.5, 4.2 Hz, 1H, CH$_{Ar}$), 6.97 (d, J = 9.0 Hz, 1H, CH$_{Ar}$), 4.47 (t, J = 2.8 Hz, 1H, CHCH$_2$CH$_2$NH), 4.15 (br s, 1H, CHCH$_2$CH$_2$NH), 4.08 (s, 7H, 7 × CH$_{Cp}$), 4.02–4.00 (m, 1H, CH$_{Cp}$), 3.76–3.74 (m, 1H, CH$_{Cp}$), 3.47–3.40 (m, 1H, CHCH$_2$(HCH)NH), 3.38–3.30 (m, 1H, CHCH$_2$(HCH)NH), 2.31–2.22 (m, 1H, CH(HCH)CH$_2$NH), 2.04 (m, 1H, CH(HCH)CH$_2$NH). ^{13}C NMR (101 MHz, CDCl$_3$) δ = 145.1 (C$_{Ar}$), 143.2 (C$_{Ar}$), 140.9 (C$_{Ar}$), 130.3 (C$_{Ar}$), 129.0 (C$_{Ar}$), 128.5 (C$_{Ar}$), 121.5 (C$_{Ar}$), 120.6 (C$_{Ar}$), 112.7 (C$_{Ar}$), 95.0 (C$_{Cp}$), 69.1 (C$_{Cp}$), 68.8 (5 × C$_{Cp}$), 67.2 (C$_{Cp}$), 66.65 (C$_{Cp}$), 66.57 (C$_{Cp}$), 37.4 (CHCH$_2$CH$_2$NH), 30.2 (CHCH$_2$CH$_2$NH), 27.8 (CHCH$_2$CH$_2$NH). IR (ATR, cm^{-1}): ν = 2926 (N–H) cm^{-1}. MS (70eV): *m/z* (%) 369.0 ([M+ H]$^+$).

*4.1.5.5. 4-Ferrocenyl-1,2,3,4-tetrahydro-1,10-phenanthroline (**8e**).* Yellow solid; mp 159 °C. Rf = 0.33 (Petroleum ether/EtOAc, 7:3 (v/v)). Yield 97%. ^{1}H NMR (400 MHz, CDCl$_3$) δ = 8.68 (dd, J = 4.2, 1.7 Hz, 1H, CH$_{Ar}$), 8.02 (dd, J = 8.3, 1.7 Hz, 1H, CH$_{Ar}$), 7.35 (d, J = 8.4 Hz, CH$_{Ar}$), 7.31 (dd, J = 8.3, 4.2 Hz, 1H, CH$_{Ar}$), 6.99 (d, J = 8.4 Hz, 1H, CH$_{Ar}$), 6.06 (s, 1H, CHCH$_2$CH$_2$NH), 4.19 (s, 5H, 5 × CH$_{Cp}$), 4.15–4.14 (m, 2H, 2 × CH$_{Cp}$), 4.08–4.05 (m, 1H, CH$_{Cp}$), 4.02 (t, J = 5.0 Hz, 1H, CHCH$_2$CH$_2$NH), 3.86–3.84 (m, 1H, CH$_{Cp}$), 3.54–3.46 (m, 1H, CHCH$_2$(HCH)NH), 3.42–3.34 (m, 1H, CHCH$_2$(HCH)NH), 2.34–2.25 (m, 1H, CH(HCH)CH$_2$NH), 2.14–2.05 (m, 1H, CH(HCH)CH$_2$NH). ^{13}C NMR (101 MHz, CDCl$_3$) δ = 146.8 (C$_{Ar}$), 140.1 (C$_{Ar}$), 137.5 (C$_{Ar}$), 135.8 (C$_{Ar}$), 129.2 (C$_{Ar}$), 127.6 (C$_{Ar}$), 120.8 (C$_{Ar}$), 118.4 (C$_{Ar}$), 112.3 (C$_{Ar}$), 94.5 (C$_{Cp}$), 69.8 (5 × C$_{Cp}$), 68.7 (C$_{Cp}$), 67.8 (C$_{Cp}$), 66.6 (C$_{Cp}$), 65.9 (C$_{Cp}$), 38.4 (CHCH$_2$CH$_2$NH), 36.4 (CHCH$_2$CH$_2$NH), 29.5 (CHCH$_2$CH$_2$NH). IR (ATR, cm^{-1}): ν = 2922 (N–H) cm^{-1}. MS (70eV): *m/z* (%) 369.0 ([M+ H]$^+$). HRMS (ESI): *m/z* for C$_{22}$H$_{20}$FeN$_2$ [M+H]$^+$ calcd 369.1049, found 369.1044.

*4.1.6. X-ray data collection and structure refinement for compounds **7d** and **8e***

Single-crystal X-ray intensity data for compounds C$_{25}$H$_{23}$F$_3$FeN$_2$O$_2$ (**7d**) and C$_{22}$H$_{20}$FeN$_2$ (**8e**) were collected on a Rigaku Oxford Diffraction SuperNova Dual Source (Cu at zero) diffractometer equipped with an Atlas CCD detector using ω scans and CuKα (λ = 1.54184 Å) radiation. The crystals were kept at 100.0(1) K during data collection. Using Olex2 [35], the structures were solved by direct methods using SHELXS and refined on F^2 by full-matrix least-squares using SHELXL [36,37]. Non-hydrogen atoms were anisotropically refined and the hydrogen atoms in the riding mode and isotropic temperature factors fixed at 1.2 times U(eq) of the parent atoms (1.5 times for methyl and hydroxyl groups). N–H and O–H hydrogen atoms were located, when possible, from a difference Fourier electron density map. Crystallographic details for structure analysis of compounds **7d** and **8e** are summarized in Table 9. (for more data see *ESI*).

4.2. Bioactivity evaluation methods

4.2.1. In vitro antimalarial assay

The test samples were prepared to a 20 mg/ml stock solution in 100% DMSO. Stock solutions were stored at −20 °C. Further dilutions were prepared in complete medium on the day of the experiment. Samples were tested as a suspension if not completely dissolved. Chloroquine (CQ) was used as the reference drugs. A full dose-response was performed to determine the concentration inhibiting 50% of parasite growth (IC$_{50}$–value). Test samples were tested at a starting concentration of 10 μg/ml (or 1 μg/ml), which was then serially diluted 2-fold in complete medium to give 10 concentrations; with the lowest concentration being 20 ng/ml (or 2 ng/ml). The same dilution technique was used for all samples. The highest concentration of solvent to which the parasites were exposed to had no measurable effect on the parasite viability (data not shown). The 50% inhibitory concentration (IC$_{50}$) values were obtained from full dose-response curves, using a non-linear dose-response curve fitting analysis *via* GraphPad Prism v.4 software.

Table 9
Crystallographic data and structure refinement for **7d** and **8e**.

Compound	**7d**	**8e**
Empirical formula	C$_{25}$H$_{23}$F$_3$FeN$_2$O$_2$	C$_{22}$H$_{20}$FeN$_2$
Formula weight	496.30	368.25
Temperature/K	100.0(1)	100.0(1)
Crystal system	Triclinic	Triclinic
Space group	P-1	P-1
a/Å	10.9525(3)	7.2660(4)
b/Å	11.6584(4)	9.2877(5)
c/Å	18.0342(5)	13.5927(7)
α/°	105.075(3)	73.730(5)
β/°	98.806(3)	79.029(4)
γ/°	90.119(3)	68.520(5)
Volume/Å3	2195.19(12)	815.44(8)
Z	4	2
P$_{calc}$g/cm^3	1.502	1.500
μ/mm^{-1}	5.960	7.441
F(000)	1024.0	384.0
Crystal size/mm^3	0.161 × 0.129 × 0.061	0.266 × 0.162 × 0.114
Radiation	CuKα (λ = 1.54184)	CuKα (λ = 1.54184)
2Θ range for data collection/°	7.862 to 150.992	6.808 to 150.658
Index ranges	−13 ≤ h ≤ 13, −14 ≤ k ≤ 14, −22 ≤ l ≤ 22	−9 ≤ h ≤ 9, −11 ≤ k ≤ 10, −17 ≤ l ≤ 17
Reflections collected	41945	15490
Independent reflections	8886 [R$_{int}$ = 0.0669, R$_{sigma}$ = 0.0527]	3315 [R$_{int}$ = 0.0463, R$_{sigma}$ = 0.0304]
Data/restraints/parameters	8886/0/599	3315/0/229
Goodness-of-fit on F^2	1.020	1.035
Final R indexes [I ≥ 2σ (I)]	R$_1$ = 0.0422, wR_2 = 0.1009	R$_1$ = 0.0289, wR_2 = 0.0772
Final R indexes [all data]	R$_1$ = 0.0572, wR_2 = 0.1101	R$_1$ = 0.0302, wR_2 = 0.0786
Largest diff. peak/hole/e Å^{-3}	0.99/-0.37	0.32/-0.54

4.2.2. In vitro assay for the evaluation of cytotoxic activity

The same stock solutions prepared for antiplasmodium testing was used for cytotoxicity testing. Test compounds were stored at −20 °C until use. Dilutions were prepared on the day of the experiment. Emetine was used as the reference drug in all experiments. The initial concentration of emetine was 100 μg/ml, which was serially diluted in complete medium with 10-fold dilutions to give 6 concentrations, the lowest being 0.001 μg/ml. The same dilution technique was applied for all test samples. The highest concentration of solvent to which the cells were exposed to had no measurable effect on the cell viability (data not shown). The 50% inhibitory concentration (IC_{50}) values were obtained from full dose-response curves, using a non-linear dose-response curve fitting analysis *via* GraphPad Prism v.4 software.

Transparency declarations

The authors declare no conflict of interest.

Supporting information

X-ray crystallographic data in CIF format, cyclic voltammograms and copies of NMR spectra for all synthesized compounds. CCDC 1953543−1953544 contain the supplementary crystallographic data for this paper and can be obtained free of charge *via* www.ccdc.cam.ac.uk/conts/retrieving.html (or from the Cambridge Crystallographic Data Centre, 12, Union Road, Cambridge CB2 1EZ, UK; fax: +44-1223-336033; or deposit@ccdc.cam.ac.uk).

Declaration of competing interest

The authors declare that they have no known competing financial interests or personal relationships that could have appeared to influence the work reported in this paper.

Acknowledgment

The authors are indebted to Ghent University (BOF) for financial support. This work was also supported by the Ministry of Education, Science and Technological Development of the Republic of Serbia (grant 172034). KVH thanks the Hercules Foundation (project AUGE/11/029 “3D-SPACE: 3D Structural Platform Aiming for Chemical Excellence”) and the Special Research Fund (BOF) − UGent (project 01N03217) for funding. The University of Cape Town, South African Medical Research Council, and South African Research Chairs Initiative of the Department of Science and Technology, administered through the South African National Research Foundation are gratefully acknowledged for support (K.C).

Appendix A. Supplementary data

Supplementary data to this article can be found online at https://doi.org/10.1016/j.ejmech.2019.111963.

References

[1] N.J. White, S. Pukrittayakamee, T.T. Hien, M.A. Faiz, O.A. Mokuolu, A.M. Dondorp, Malaria, Lancet 383 (2014) 723−735, https://doi.org/10.1016/S0140-6736(13)60024-0.
[2] K. Mendis, B. Sina, P. Marchesini, R. Carter, The neglected burden of *Plasmodium vivax* malaria, Am. J. Trop. Med. Hyg. 64 (2001) 97−106, https://doi.org/10.4269/ajtmh.2001.64.97.
[3] S. Vandekerckhove, M. D'hooghe, Quinoline-based antimalarial hybrid compounds, Bioorg. Med. Chem. 23 (2015) 5098−5119, https://doi.org/10.1016/j.bmc.2014.12.018.
[4] S. Vandekerckhove, S. Van Herreweghe, J. Willems, B. Danneels, T. Desmet, C. de Kock, P.J. Smith, K. Chibale, M. D'hooghe, Synthesis of functionalized 3-, 5-, 6- and 8-aminoquinolines *via* intermediate (3-pyrrolin-1-yl)- and (2-oxopyrrolidin-1-yl)quinolines and evaluation of their antiplasmodial and antifungal activity, Eur. J. Med. Chem. 92 (2015) 91−102, https://doi.org/10.1016/j.ejmech.2014.12.020.
[5] R.A. Jones, S.S. Panda, C.D. Hall, Quinine conjugates and quinine analogues as potential antimalarial agents, Eur. J. Med. Chem. 97 (2015) 335−355, https://doi.org/10.1016/j.ejmech.2015.02.002.
[6] Africa WHO, World Health Organisation, Malaria Report 2003, Geneva, 2003.
[7] World WHO, World Health Organisation, Malaria Report 2018, Geneva, 2018.
[8] B. Greenwood, The contribution of vaccination to global health: past, present and future, Phil. Trans. R. Soc. B 369 (2014) 20130433, https://doi.org/10.1098/rstb.2013.0433.
[9] D. Gambino, L. Otero, Perspectives on what ruthenium-based compounds could offer in the development of potential antiparasitic drugs, Inorg. Chim. Acta 393 (2012) 103−114, https://doi.org/10.1016/j.ica.2012.05.028.
[10] P.F. Salas, C. Herrmann, C. Orvig, Metalloantimalarials, Chem. Rev. 113 (2013) 3450−3492, https://doi.org/10.1021/cr3001252.
[11] C. Biot, W. Castro, C.Y. Botte, M. Navarro, The therapeutic potential of metal-based antimalarial agents: implications for the mechanism of action, Dalton Trans. 41 (2012) 6335−6349, https://doi.org/10.1039/C2DT12247B.
[12] M. Navarro, W. Castro, C. Biot, Bioorganometallic compounds with antimalarial targets: inhibiting hemozoin formation, Organometallics 31 (2012) 5715−5727, https://doi.org/10.1021/om300296n.
[13] G. Mombo-Ngoma, C. Supan, M.P. Dal-Bianco, M.A. Missinou, P.B. Matsiegui, C.L.O. Salazar, S. Issifou, D. Ter-Minassian, M. Ramharter, M. Kombila, P.G. Kremsner, B. Lell, Phase I randomized dose-ascending placebo-controlled trials of ferroquine - a candidate anti-malarial drug - in adults with asymptomatic *Plasmodium falciparum* infection, Malar. J. 10 (2011) 53, https://doi.org/10.1186/1475-2875-10-53.
[14] C. Supan, G. Mombo-Ngoma, M.P. Dal-Bianco, C.L.O. Salazar, S. Issifou, F. Mazuir, A. Filali-Ansary, C. Biot, D. Ter-Minassian, M. Ramharter, P.G. Kremsner, B. Lell, Pharmacokinetics of ferroquine, a novel 4-aminoquinoline, in asymptomatic carriers of *Plasmodium falciparum* infections, Antimicrob. Agents Chemother. 56 (2012) 3165−3173, https://doi.org/10.1128/AAC.05359-11.
[15] D. Dive, C. Biot, Ferrocene conjugates of chloroquine and other antimalarials: the development of ferroquine, a new antimalarial, ChemMedChem 3 (2008) 383−391, https://doi.org/10.1002/cmdc.200700127.
[16] D. N'Da, P. Smith, Synthesis, *in vitro* antiplasmodial and antiproliferative activities of a series of quinoline-ferrocene hybrids, Med. Chem. Res. 23 (2014) 1214−1224, https://doi.org/10.1007/s00044-013-0748-4.
[17] I. Damljanović, D. Stevanović, A. Pejović, M. Vukićević, S.B. Novaković, G.A. Bogdanović, T. Mihajilov-Krstev, N. Radulović, R.D. Vukićević, Antibacterial 3-(arylamino)-1-ferrocenylpropan-1-ones: synthesis, spectral, electrochemical and structural characterization, J. Organomet. Chem. 696 (2011) 3703−3713, https://doi.org/10.1016/j.jorganchem.2011.08.016.
[18] A. Pejović, D. Stevanović, I. Damljanović, M. Vukićević, S.B. Novaković, G.A. Bogdanović, T. Mihajilov-Krstev, N. Radulović, R.D. Vukićević, Ultrasound-assisted synthesis of 3-(Arylamino)-1-ferrocenylpropan-1-ones, Helv. Chim. Acta 95 (2012) 1425−1441, https://doi.org/10.1002/hlca.201200009.
[19] A. Minić, D. Stevanović, I. Damljanović, A. Pejović, M. Vukićević, G.A. Bogdanović, N.S. Radulović, R.D. Vukićević, Synthesis of ferrocene-containing six-membered cyclic ureas *via* α-ferrocenyl carbocations, RSC Adv. 5 (2015) 24915−24919, https://doi.org/10.1039/c5ra01383f.
[20] A. Minić, D. Stevanović, M. Vukićević, G.A. Bogdanović, M. D'hooghe, N.S. Radulović, R.D. Vukićević, Synthesis of novel 4-ferrocenyl-1,2,3,4-tetrahydroquinolines and 4-ferrocenylquinolines *via* α-ferrocenyl carbenium ions as key intermediates, Tetrahedron 73 (2017) 6268−6274, https://doi.org/10.1016/j.tet.2017.09.014.
[21] **8a** - 4-Ferrocenyl-1,2,3,4-tetrahydrobenzo[h][1,6]naphthyridine; **8b** - 1-Ferrocenyl-1,2,3,4-tetrahydrobenzo[f][1,7]naphthyridine; **8c** - 4-Ferrocenyl-1,2,3,4-tetrahydro-1,7-phenanthroline; **8d** - 1-Ferrocenyl-1,2,3,4-tetrahydro-4,7-phenanthroline; **8e** - 4-Ferrocenyl-1,2,3,4-tetrahydro-1,10-phenanthroline.
[22] X.-J. Tang, Z.-L. Yan, W.-L. Chen, Y.-R. Gao, S. Mao, Y.-L. Zhang, Y.-Q. Wang, Aza-Michael reaction promoted by aqueous sodium carbonate solution, Tetrahedron Lett. 54 (2013) 2669−2673, https://doi.org/10.1016/j.tetlet.2013.03.043.
[23] A. Pejović, B. Danneels, T. Desmet, B.T. Cham, T. Nguyen, N.S. Radulović, R.D. Vukićević, M. D'hooghe, Synthesis and antimicrobial/cytotoxic assessment of ferrocenyl oxazinanes, oxazinan-2-ones, and tetrahydropyrimidin-2-ones, Synlett 26 (2015) 1195−1200, https://doi.org/10.1055/s-0034-1380348.
[24] A. Minić, J. Bugarinović, A. Pejović, D. Ilić-Komatina, G.A. Bogdanović, I. Damljanović, D. Stevanović, Synthesis of novel ferrocene-containing 1,3-thiazinan-2-imines: one-pot reaction promoted by ultrasound irradiation, Tetrahedron Lett. 59 (2018) 3499−3502, https://doi.org/10.1016/j.tetlet.2018.08.029.
[25] A. Pejović, A. Minić, J. Bugarinović, M. Pešić, I. Damljanović, D. Stevanović, V. Mihailović, J. Katanić, G.A. Bogdanović, Synthesis, characterization and antimicrobial activity of novel 3-ferrocenyl-2-pyrazolyl-1,3-thiazolidin-4-ones, Polyhedron 155 (2018) 382−389, https://doi.org/10.1016/j.poly.2018.08.071.
[26] Z.R. Ratković, Z.D. Juranić, T.P. Stanojković, D.D. Manojlović, R.D. Vukićević, N.S. Radulović, M.D. Joksović, Synthesis, characterization, electrochemical studies and antitumor activity of some new chalcone analogues containing ferrocenyl pyrazole moiety, Bioorg. Chem. 38 (2010) 26−32, https://doi.org/

10.1016/j.bioorg.2009.09.003.
[27] G. Elmas, A. Okumus, L.Y. Koç, H. Soltanzade, Z. Kılıç, T. Hökelek, H. Dal, L. Açık, Z. Üstündag, D. Dündar, M. Yavuz, Phosphorusenitrogen compounds. Part 29. Syntheses, crystal structures, spectroscopic and stereogenic properties, electrochemical investigations, antituberculosis, antimicrobial and cytotoxic activities and DNA interactions of ansa-spiro-ansa cyclotetraphosphazenes, Eur. J. Med. Chem. 87 (2014) 662–676, https://doi.org/10.1016/j.ejmech.2014.10.005.
[28] R. Chopra, C. de Kock, P. Smith, K. Chibale, K. Singh, Ferrocene-pyrimidine conjugates: synthesis, electrochemistry, physicochemical properties and antiplasmodial activities, Eur. J. Med. Chem. 100 (2015) 1–9, https://doi.org/10.1016/j.ejmech.2015.05.043.
[29] A. Pejović, I. Damljanović, D. Stevanović, A. Minić, J. Jovanović, V. Mihailović, J. Katanić, G.A. Bogdanović, Synthesis, characterization and antimicrobial activity of novel ferrocene containing quinolines: 2-ferrocenyl-4-methoxyquinolines, 1-benzyl-2-ferrocenyl-2,3-dihydroquinolin-4(1*H*)-ones and 1-benzyl-2-ferrocenylquinolin-4(1*H*)-ones, J. Organomet. Chem. 846 (2017) 6–17, https://doi.org/10.1016/j.jorganchem.2017.05.051.
[30] A.J. Bard, L.R. Faulkner, Electrochemical Methods: Fundamentals and Applications, second ed., John Wiley and Sons, Inc, Hoboken, 2001, ISBN 0-471-04372-9.
[31] W. Trager, J.B. Jensen, Human malaria parasites in continuous culture, Science 193 (1976) 673–675, https://doi.org/10.1126/science.781840.
[32] M.T. Makler, J.M. Ries, J.A. Williams, J.E. Bancroft, R.C. Piper, B.L. Gibbins, D.J. Hinrichs, Parasite lactate dehydrogenase as an assay for *Plasmodium falciparum* drug sensitivity, Am. J. Trop. Med. Hyg. 48 (1993) 739–741, https://doi.org/10.4269/ajtmh.1993.48.739.
[33] T. Mosmann, Rapid colorimetric assay for cellular growth and survival: application to proliferation and cytotoxicity assays, J. Immunol. Methods 65 (1983) 55–63, https://doi.org/10.1016/0022-1759(83)90303-4.
[34] L.V. Rubinstein, R.H. Shoemaker, K.D. Paull, R.M. Simon, S. Tosini, P. Skehan, D.A. Scudiero, A. Monks, M.R. Boyd, Comparison of *in vitro* anticancer-drug-screening data generated with a tetrazolium assay versus a protein assay against a diverse panel of human tumor cell lines, J. Natl. Cancer Inst. 82 (1990) 1113–1117, https://doi.org/10.1093/jnci/82.13.1113.
[35] O.V. Dolomanov, L.J. Bourhis, R. J Gildea, J.A.K. Howard, H. Puschmann, OLEX2: a complete structure solution, refinement and analysis program, J. Appl. Crystallogr. 42 (2009) 339–341, https://doi.org/10.1107/S0021889808042726.
[36] G.M. Sheldrick, A short history of *SHELX*, Acta Crystallogr. A64 (2008) 112–122, https://doi.org/10.1107/S0108767307043930.
[37] G.M. Sheldrick, Crystal structure refinement with *SHELXL*, Acta Crystallogr. C71 (2015) 3–8, https://doi.org/10.1107/S2053229614024218.